DE LA RECHERCHE À L'INDUSTRIE

www.cea.fr

1880

Professor Mayer's topophone

Today

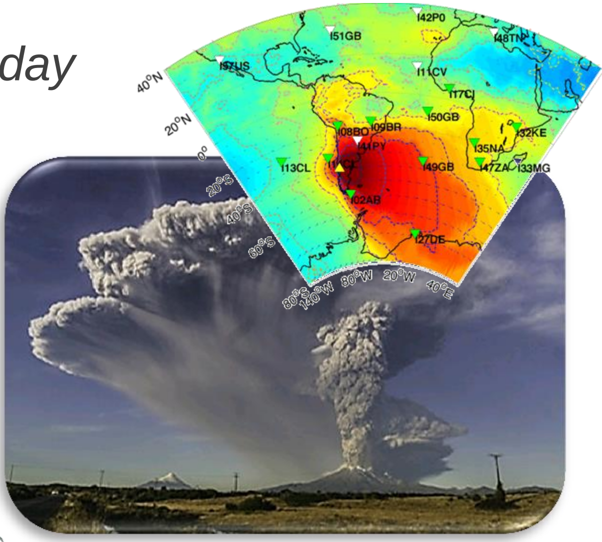

Calbuco eruption, Chile (April 2015)

Infrasound for verification technology and beyond

CEA DAM DI F-91297 Arpajon France
alexis.le-pichon@cea.fr

The early history of infrasound

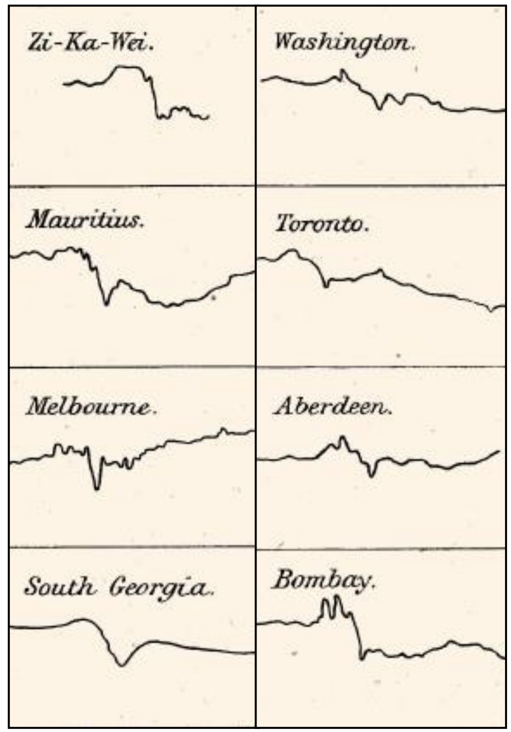

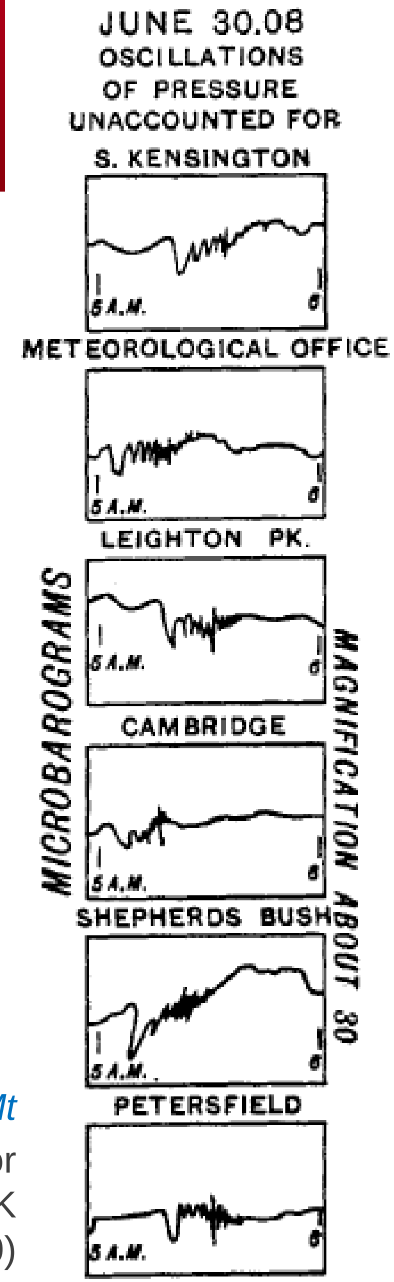

FIG. 1. — Oscillations over the region from Cambridge to Petersfield, June 30, 1908.

Eruption of Krakatoa (May, 1883)

1888 Lithograph - Parker & Coward

Barograms from all over the world showing the disturbances caused by the eruption (Symons, 1888)

The great Siberian meteor (June, 1908), ~10 Mt

Oscillations from the Tunguska meteor observed on microbarographs in the UK (Whipple, 1930)

The early history of infrasound

1920-1940

http://www.aqpl43.dsl.pipex.com/MUSEU/COMMS/ear/ear.htm

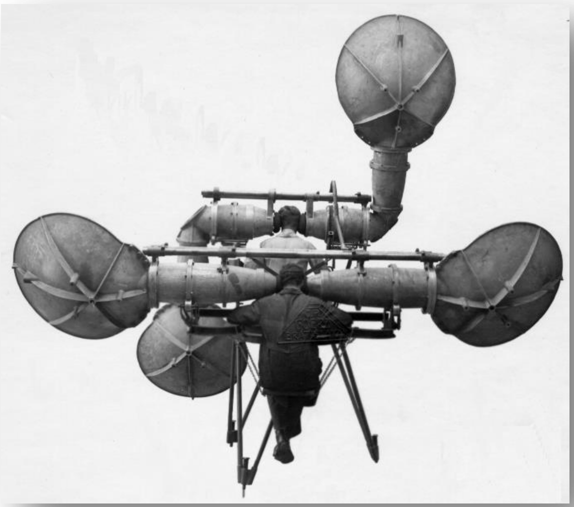

Czech four-horn height locator: 1920s

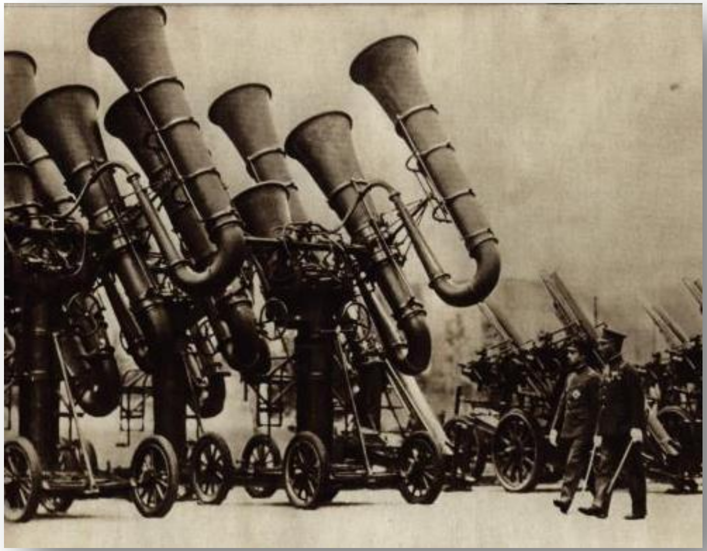

Japanese war-tubas: 1930s

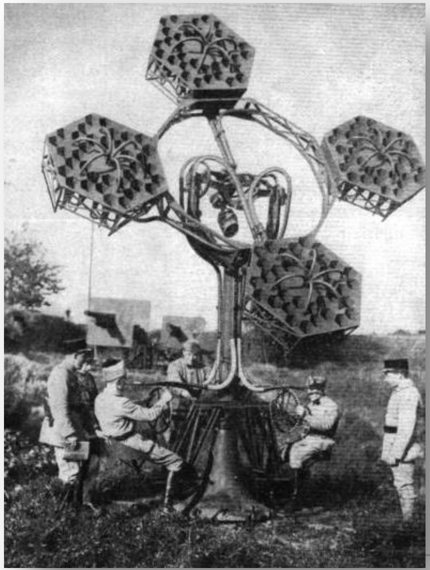

Acoustic locator on trial in France: 1930s.

US Army sound locator:1943

From atmospheric nuclear tests to IMS infrasound era

IMS: International Monitoring System

1950-1970: studying signals from large explosions and atmospheric nuclear tests

(e.g. Benioff, 1939; Rocard, 1959; Posey, 1971; Flores, 1975)

First microbarometer (CEA, 1956)

Examples of signals in French Polynesia

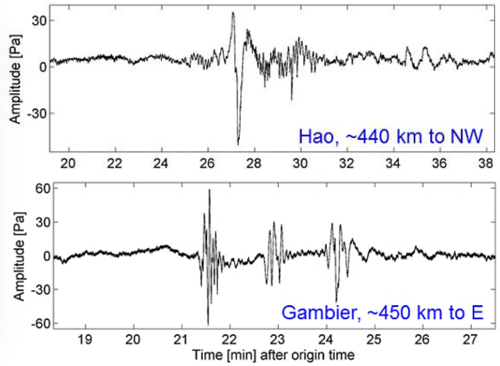

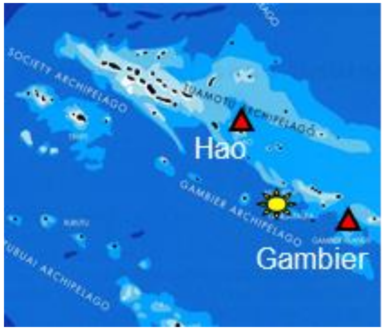

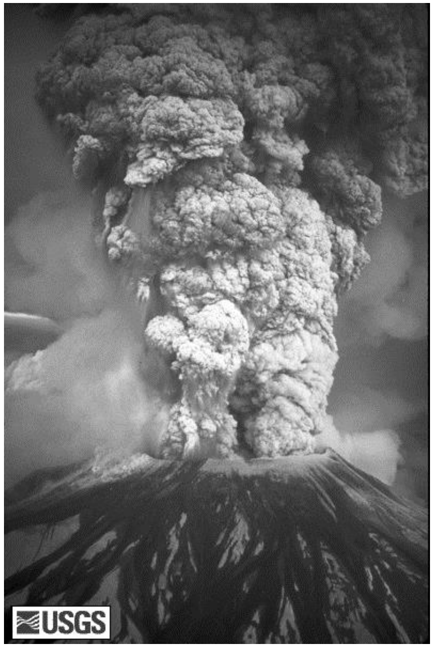

1963: Limited Test Ban Treaty, infrasound research slowed with a reduced number of studied reference events:

- explosive tests *(e.g. Al'Perovich, 1985; Whitaker, 1990)*
- industrial accidents *(e.g. Grover, 1974)*
- large natural events *(e.g. Donn, 1981; Delclos et al., 1990)*

…

From atmospheric nuclear tests to IMS infrasound era

Since 1994: rapid advance in infrasound monitoring technology

- Geneva Conference on Disarmament (1994) – IMS
- CTBT opened for signature (1996)
- Highly sensitive sensors and noise filtering systems
- Advances in array designs and processing methods
- Propagation and network performance modeling

IMS network

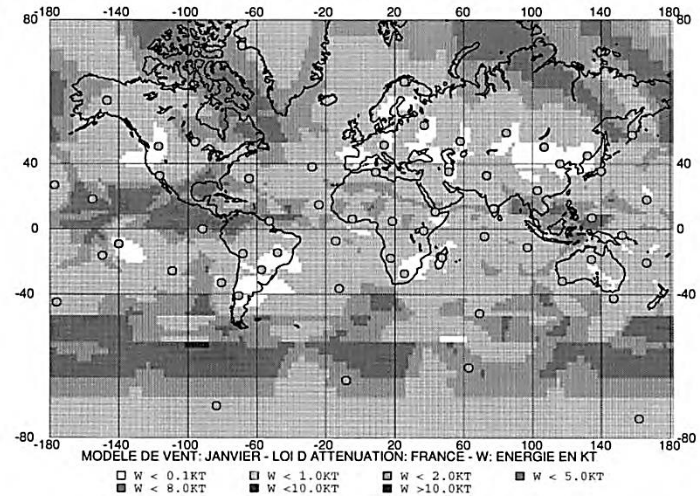

Nuclear Test Ban Working Group on Verification (CEA, 1995)

Microbarometer + acoustic filter

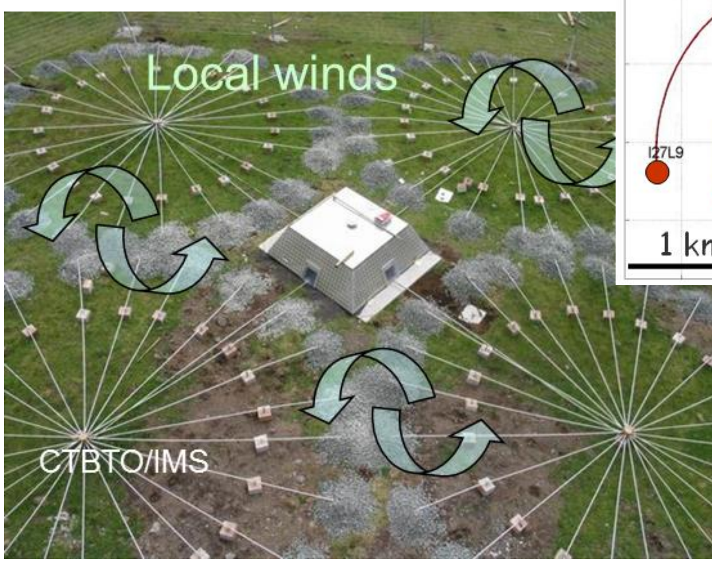

Array of microbarometers

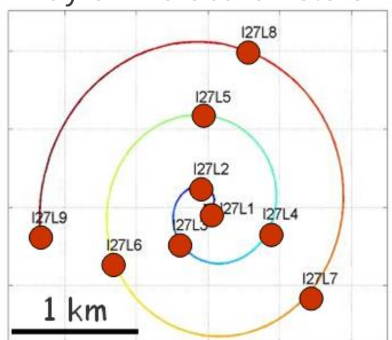

MB2005
DC-27 Hz
Noise 2 mPa rms

Dynamic wave activity, from Hz to days (Hupe, 2018)

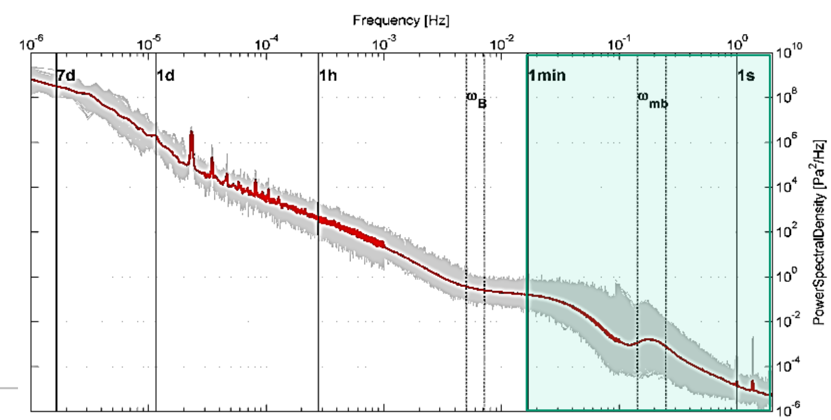

IMS infrasound network today

- International Monitoring System (IMS)
  - Operational global network of 60 infrasound arrays
  - ~80% operating stations
  - Already allows studies on a global scale
- A “zoo” of infrasound sources (0.02-4 Hz)
  - Ocean waves, explosions, bolides, earthquakes, volcanoes, hurricanes…
- An opportunity to calibrate the network and promote civil and scientific applications

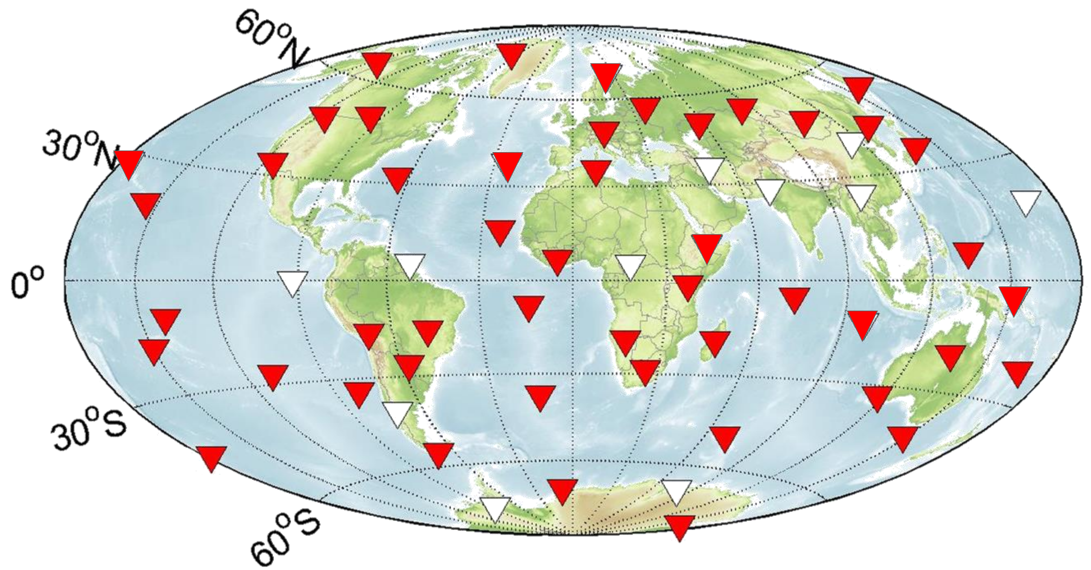

Outline

- Main challenges for infrasound interpretation
  - Highly variable atmospheric conditions
  - Improve knowledge on station signatures for discrimination
- Propagation and source studies
  - Using reference sources to assess atmospheric models
  - Network performance modeling
  - Earthquake generated infrasound
- Potential benefit for civil and scientific applications
  - Geophysical hazard warning systems
  - Developing atmospheric remote sensing method using infrasound
  - Towards a multi-technology approach to improve knowledge of the middle and upper atmosphere

Main challenge for infrasound interpretation
Highly variable station noise

- ❑ Highly variable wind-, site-, time- and frequency-dependent station noise
- ❑ Seasonal/daily variations of station detection capability

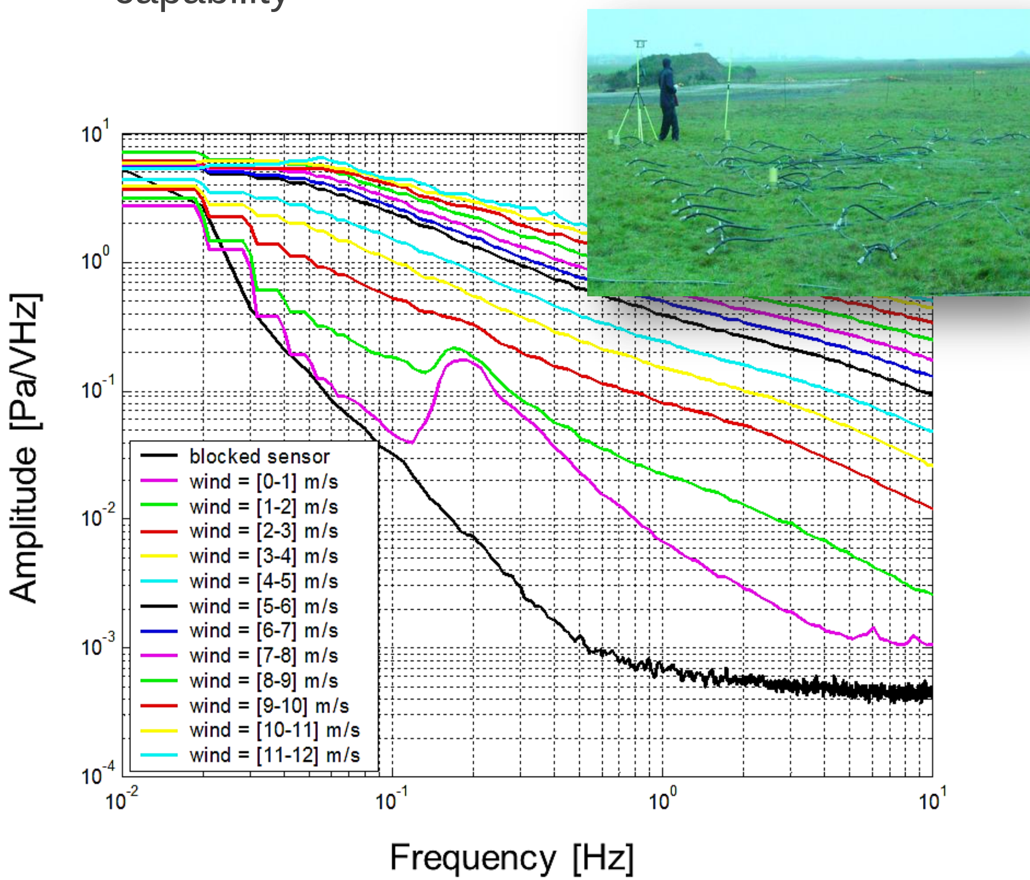

Yearly averaged PSD – 48 IMS stations

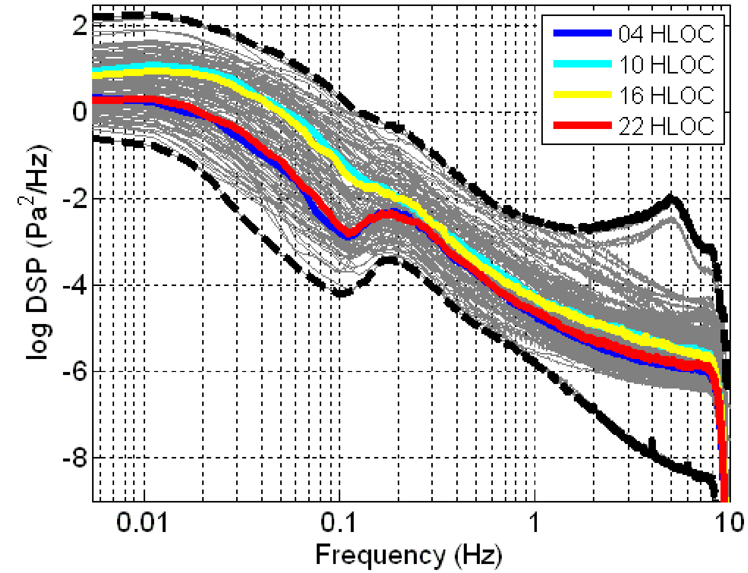

IS08 – Bolivia (2017)

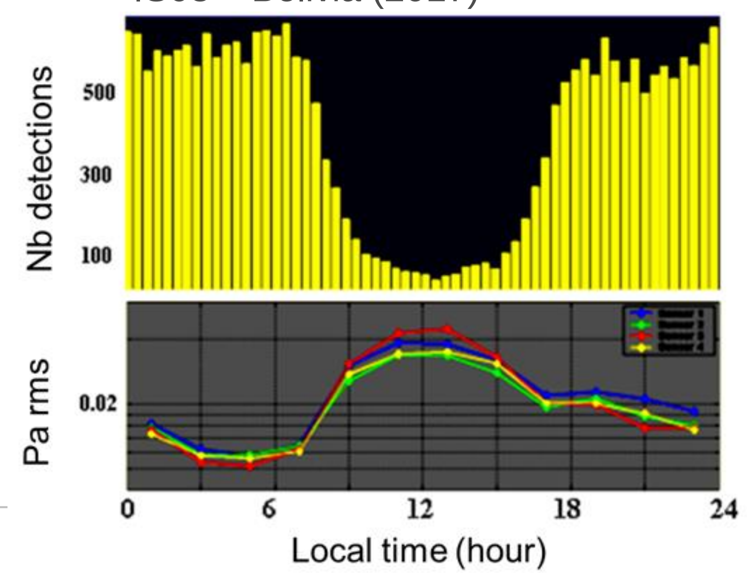

IS17- Ivory Coast

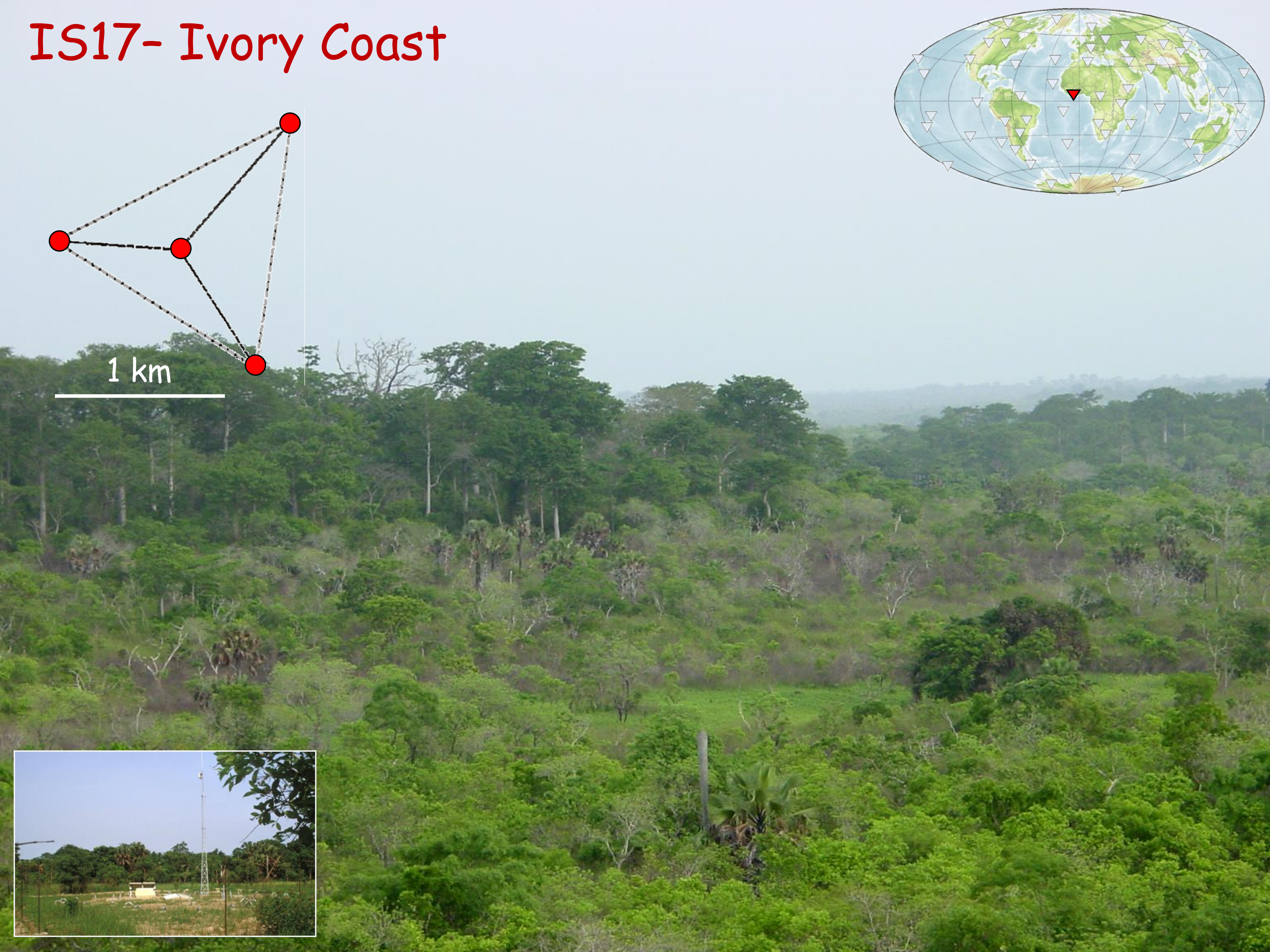

Main challenge for infrasound interpretation
Improving noise reducer system

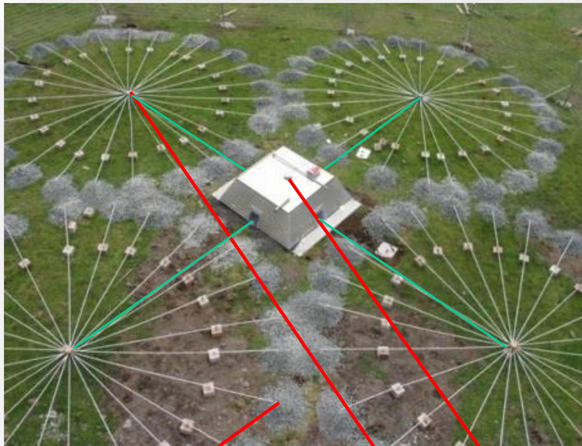

inlet and pipe

cavity and pipe

sensor

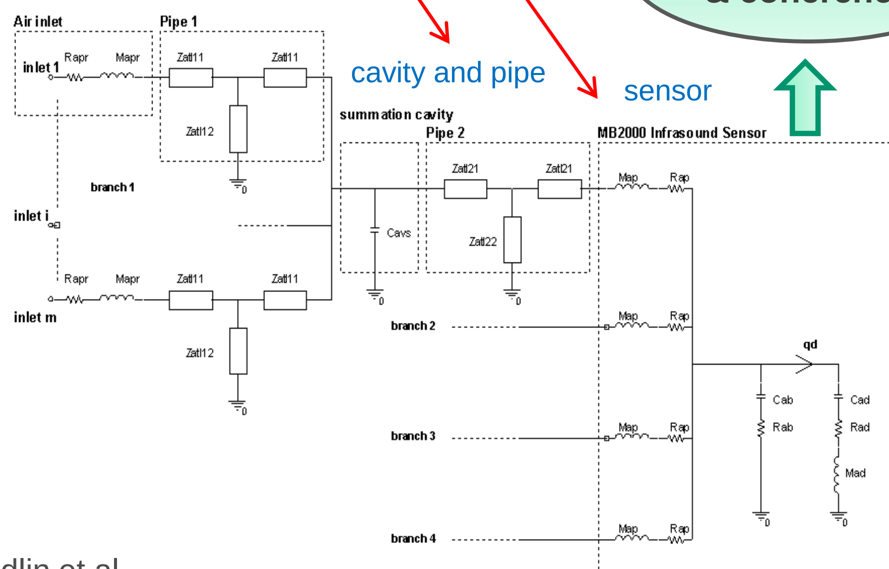

Geometrical parameters:

Number of inlets and pipes
Geometry

Construction parameters:

Length of pipes
Diameter of pipes
Volumes of manifolds
Model of sensor used

➔ **Electro-acoustic model**

Wind noise & coherence

Frequency response (dB)

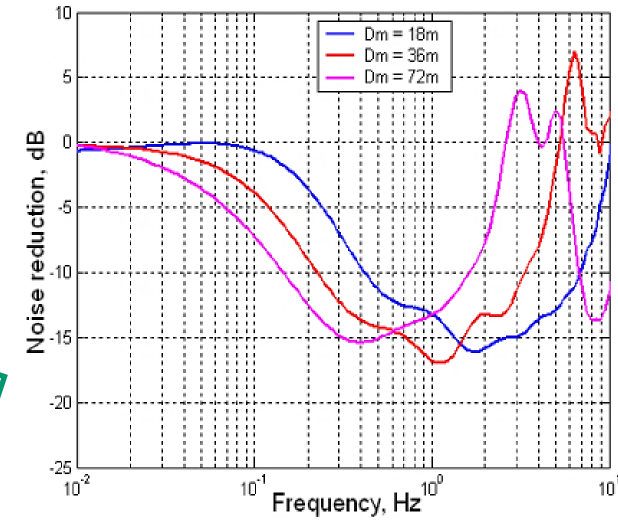

- ❑ Spatial averaging using low-impedance inlets
- ❑ Optimize cost-effective design
- ❑ Adjust diameter to local wind speed
- ❑ Adjust length of the pipes to shift resonances
- ❑ Improve SNR by ~15 dB

➔ Low acoustic impedance system used at IMS stations

Hedlin et al.
Springer, 2010

IS22– New Caledonia

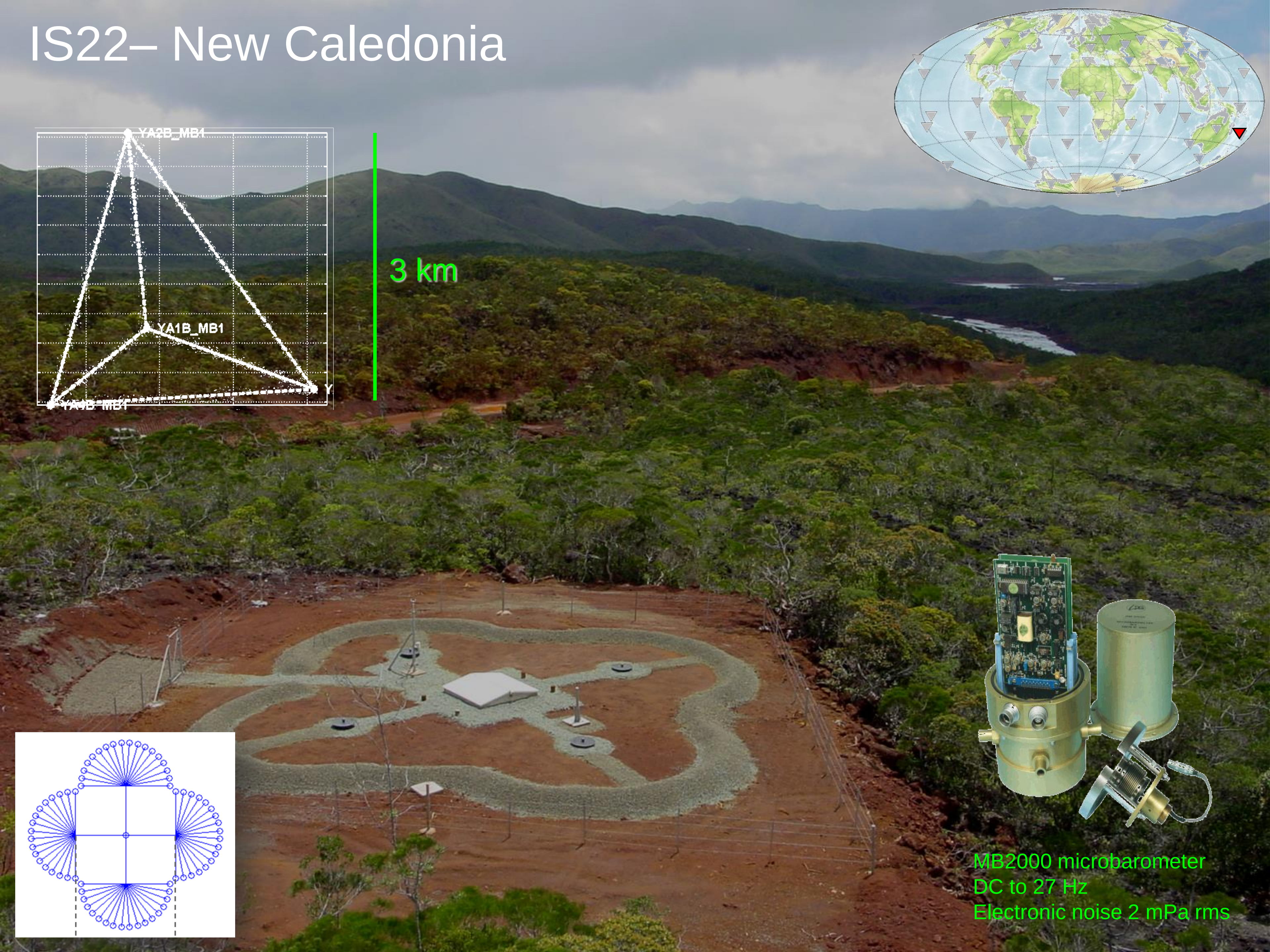

Main challenge for infrasound interpretation
Detecting low-amplitude signals (SNR<1)

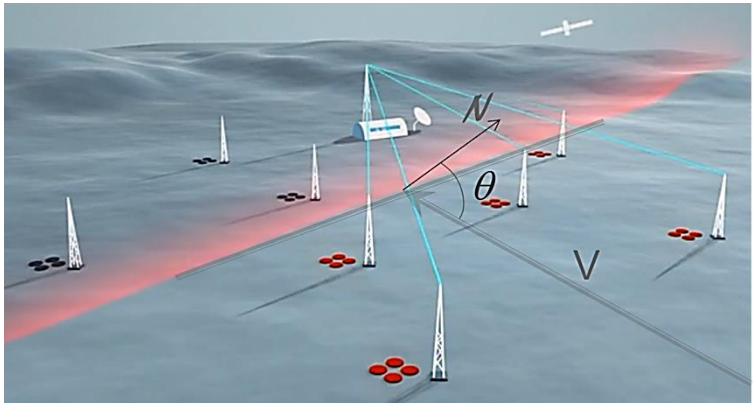

PMCC = Progressive MultiChannel Correlation (Cansi, 1995)

- Time-domain correlation method
  - filtered signals (narrow bands)

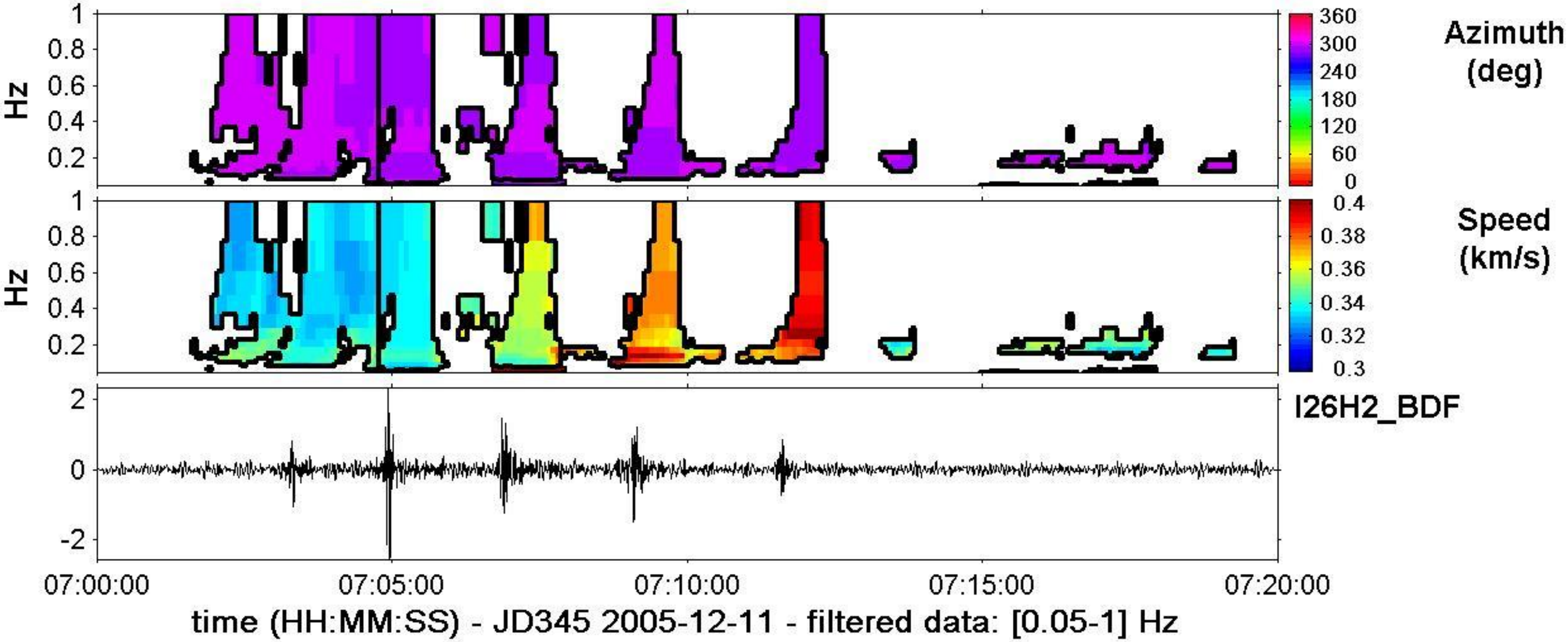

Main challenge for infrasound interpretation

A zoo of signals of natural origin

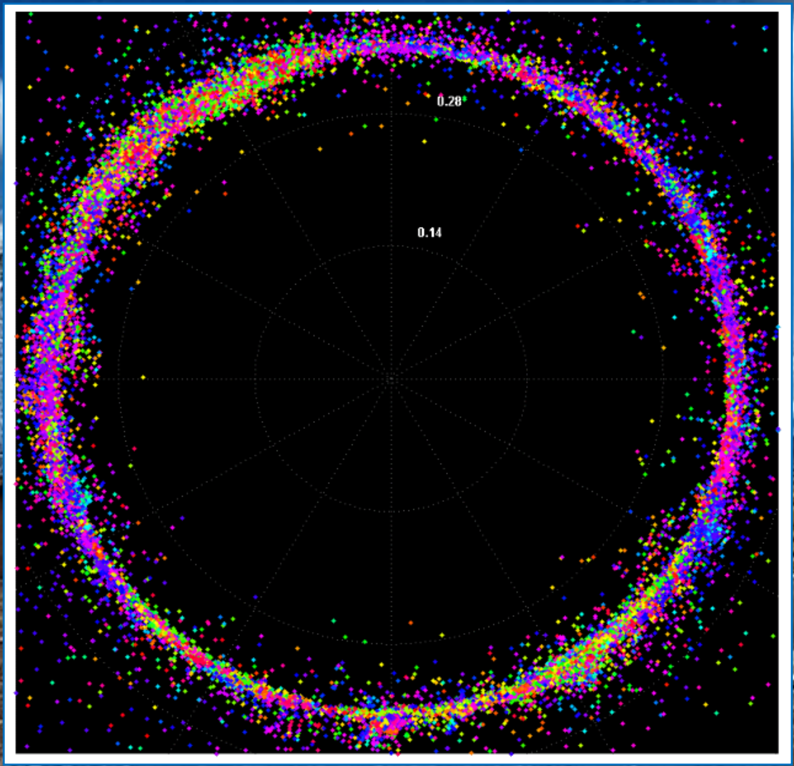

IS08 – Bolivia (2017)
~33,000 detections

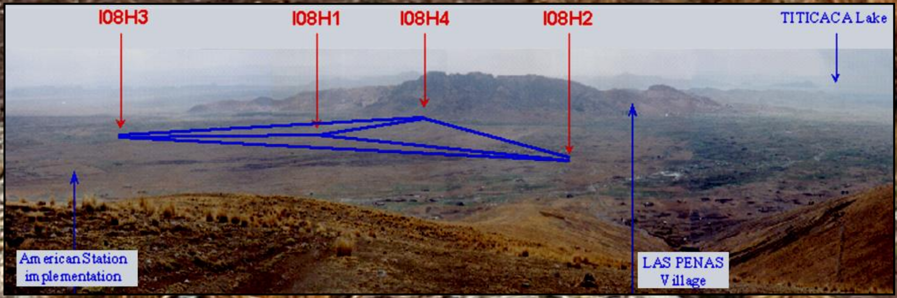

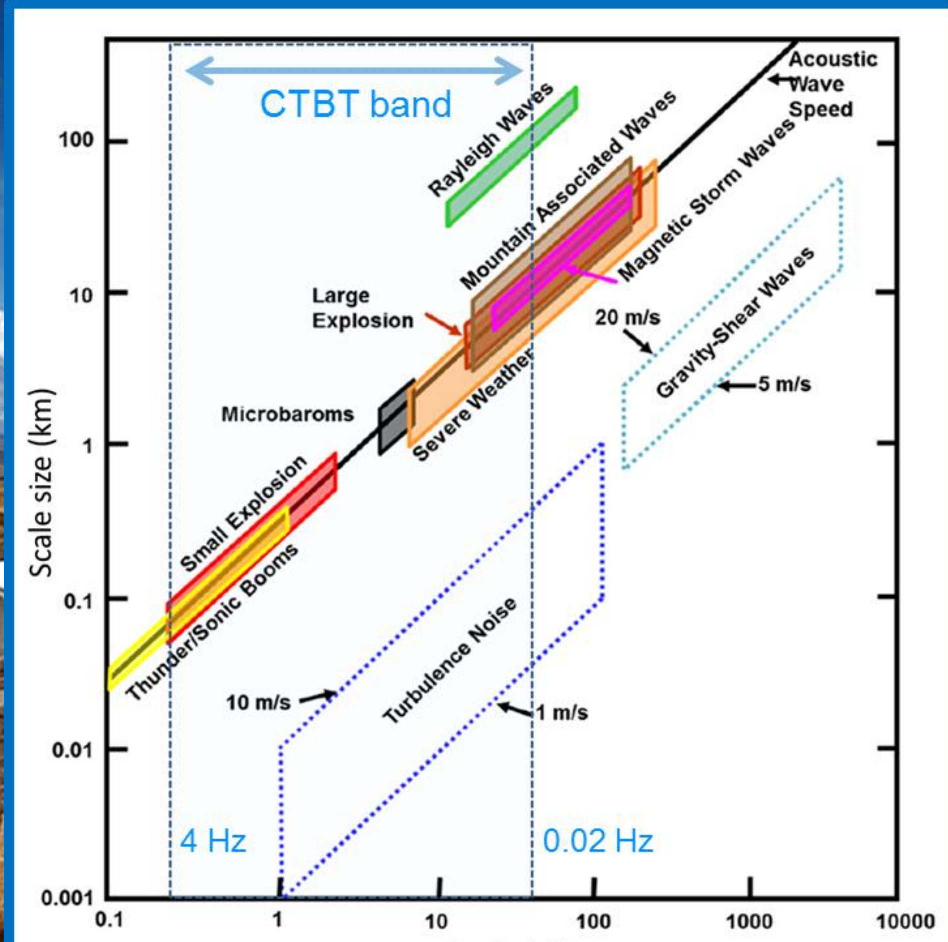

Silber and Brown, 2014

Implementing an adaptive frequency bands allows a better discrimination between interfering signals

Main challenge for infrasound interpretation
Highly variable atmospheric conditions

- Highly variable winds in strength and direction
- Zonal stratospheric winds produce efficient ducting for long propagation range

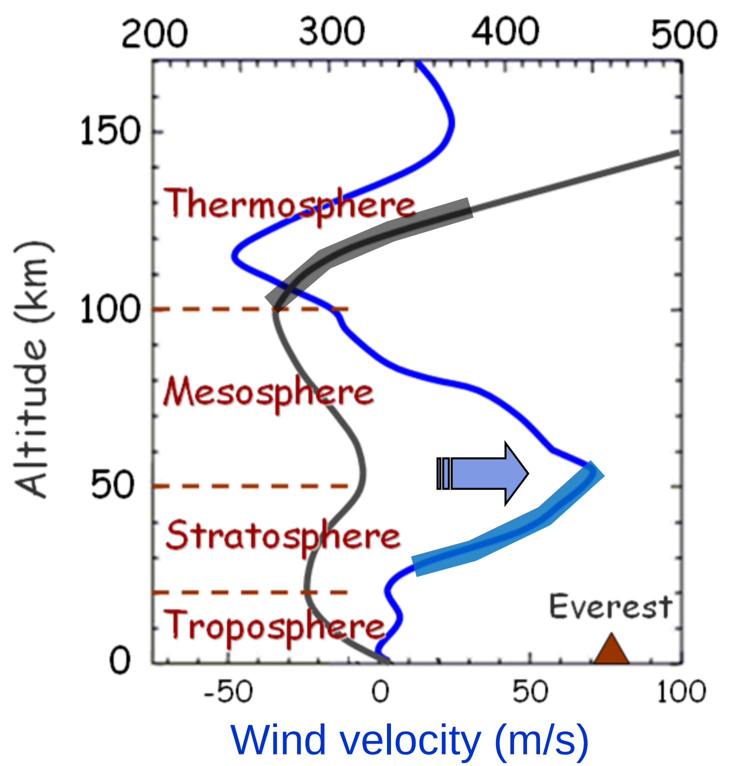

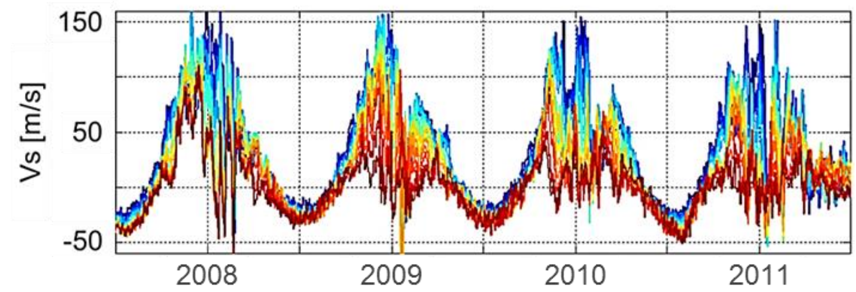

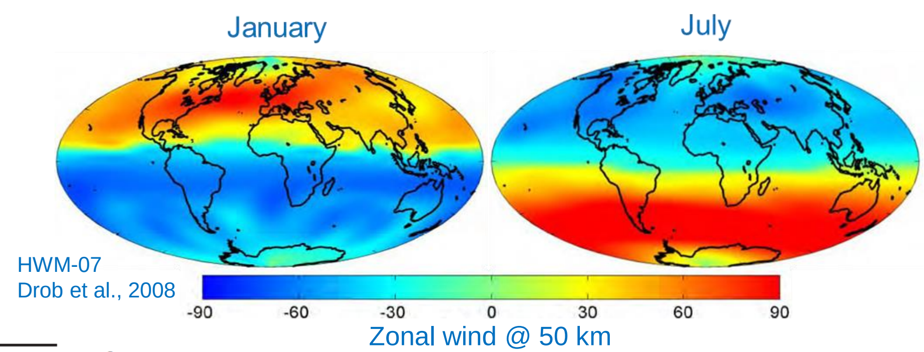

$$c_{eff} = \sqrt{\gamma_g R T} + \hat{n} \cdot \mathbf{u}$$

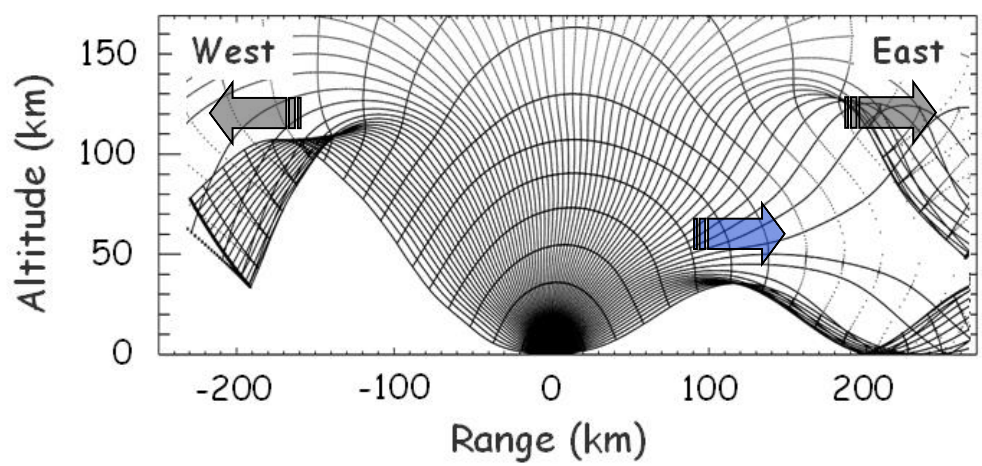

Outline

- ❑ Main challenges for infrasound interpretation
  - Highly variable atmospheric conditions
  - Improve knowledge on station signatures for discrimination
- ❑ Propagation and source studies
  - Using reference sources to assess atmospheric models
  - Network performance modeling
  - Earthquake generated infrasound
- ❑ Potential benefit for civil and scientific applications
  - Geophysical hazard warning systems
  - Developing atmospheric remote sensing method using infrasound
  - Towards a multi-technology approach to improve knowledge of the middle and upper atmosphere

From climatology to semi-empirical atmospheric models

Example of the Buncefield oil depot explosion

- 11-Dec-2005 06:01:32 (UTC)
- 51.78N / 0.43W (source: BGS)
- Hemel Hempstead, 40 km north of London
- vapor cloud blew up (~80,000 m^2 and 1 to 7 m thick, ~300 t)
- generated infrasound recorded all over Europe

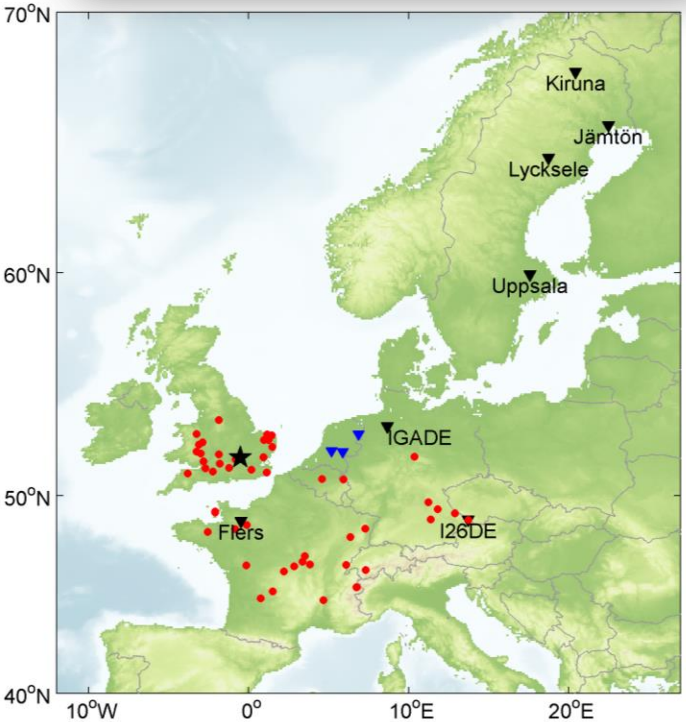

I26DE – 1057 km

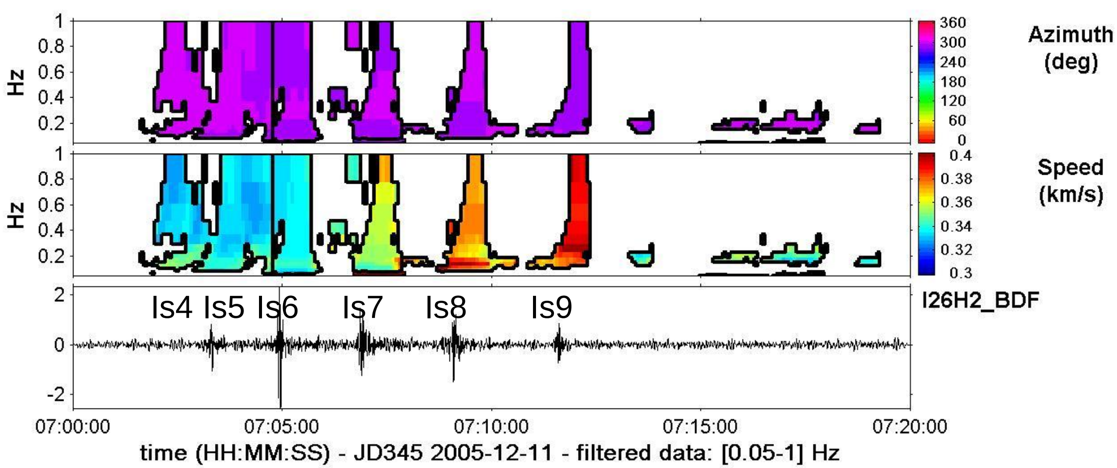

The Buncefield explosion
Interpretation / extracting mean features – NLR-G2S

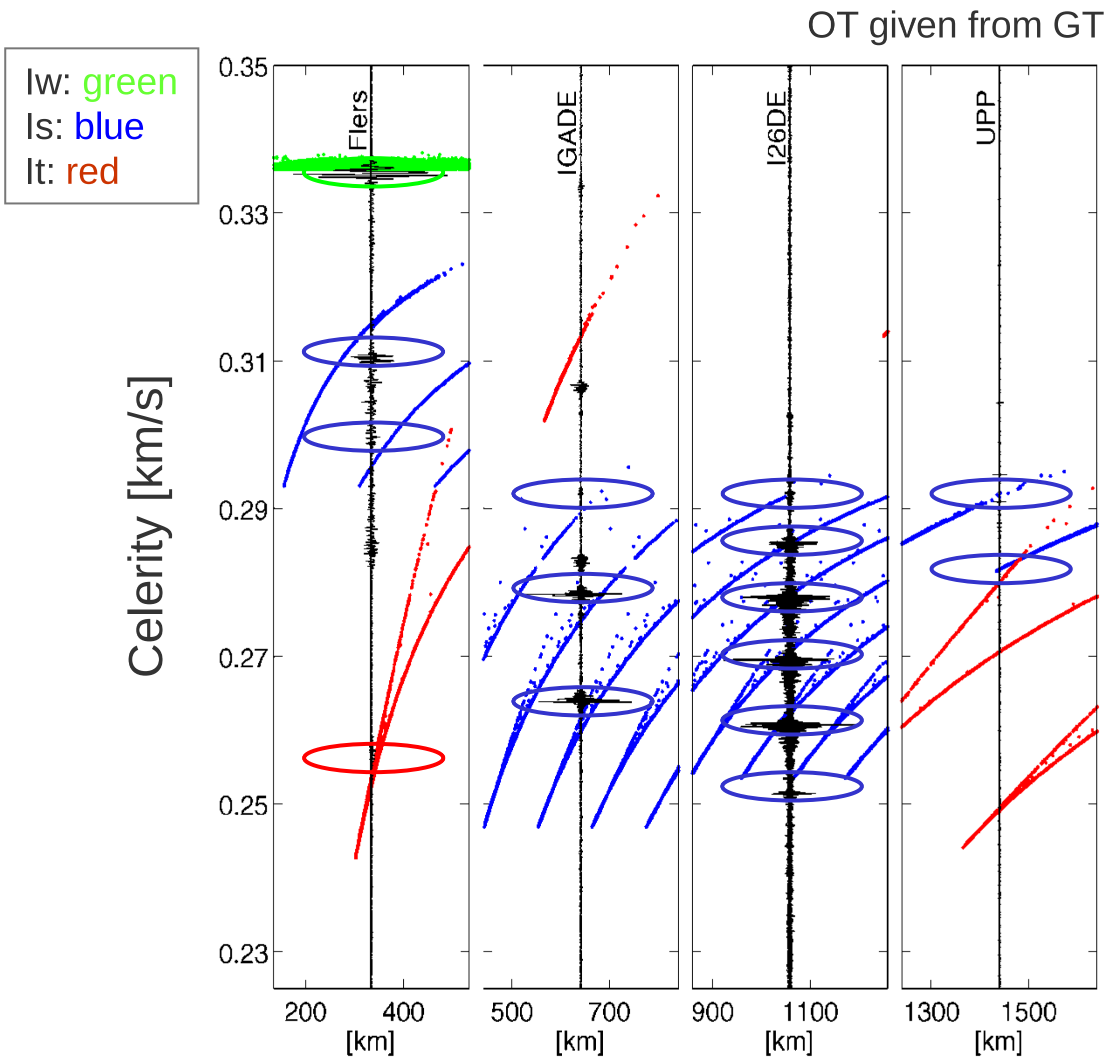

Flers

- Iw 06:18:20 β=-0.1° δβ=0.3°
- Is 06:19:54 β=3.4° δβ=-1.9°
- $(Is)_2$ 06:21:13 β=2.9° δβ=-1.9°
- It 06:24:11 β=9.0° δβ=-7.1°

IGADE

- $(Is)_3$ 06:38:17 β=255.7° δβ=5.9°
- $(Is)_4$ 06:40:28 β=252.9° δβ=5.9°
- $(Is)_5$ 06:42:32 β=252.0° δβ=5.9°

I26DE

- $(Is)_4$ 07:01:52 β=294.4° δβ=1.0°
- $(Is)_5$ 07:03:19 β=292.5° δβ=1.2°
- $(Is)_6$ 07:04:57 β=292.6° δβ=1.3°
- $(Is)_7$ 07:06:56 β=291.7° δβ=1.4°
- $(Is)_8$ 07:09:12 β=291.3° δβ=1.6°
- $(Is)_9$ 07:11:39 β=291.6° δβ=1.8°

Uppsala

- $(Is)_7$ 07:22:28 β=228.2° δβ=8.5°
- $(Is)_8$ 07:26:23 β=230.6° δβ=8.5°

➔ NRL-G2S specifications (Drob et al., 2003) explain 15 phases

Ceranna et al., JGI, 2009

The Buncefield explosion
Localization – HWM vs. NRL-G2S

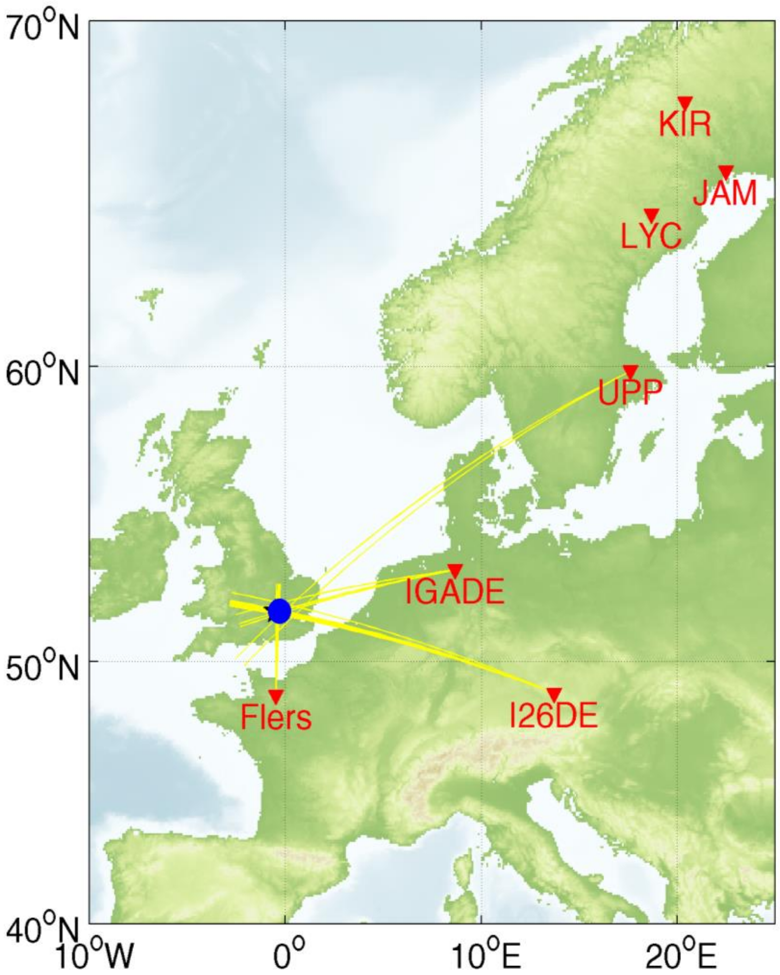

11-Dec-2005 06:05:17
51.45° N / 0.49°E
Δ = 74 km
Δt = 230 s

11-Dec-2005 06:01:55
51.73° N / 0.33°W
Δ = 8 km
Δt = 23 s

- Benchmark for operational monitoring methods (signal processing, propagation, phase labeling and localization procedure)
- Improve source location using wind corrected and phase dependent travel time curves
- Elaborate time-space dependent travel-time curves used for operational monitoring

Ceranna et al., JGI, 2009

Modeling the detection capability of the global IMS network

- Frequency dependent semi-empirical attenuations
- Atmospheric specifications (ECMWF IFS)
- Measured background station noise (Brown et al., 2014)

➔ Overall, a 1 kt explosion would be detected at any time of the year

➔ Implemented in automatic procedures: daily maps

➔ Optimize network

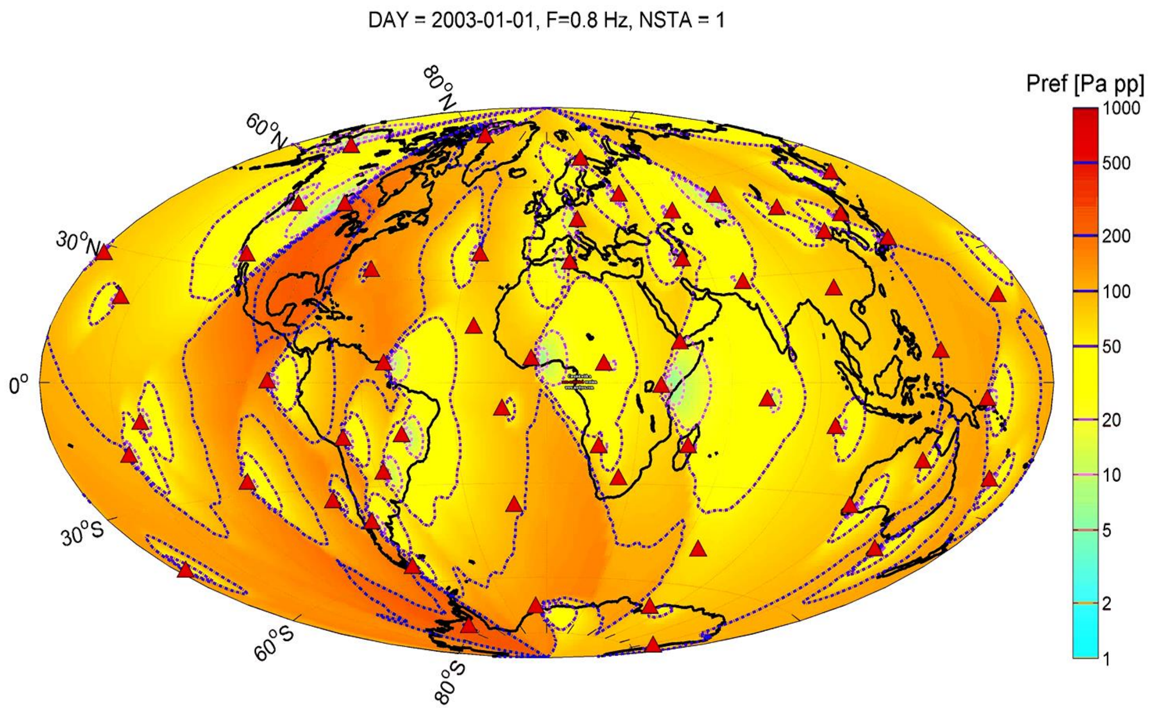

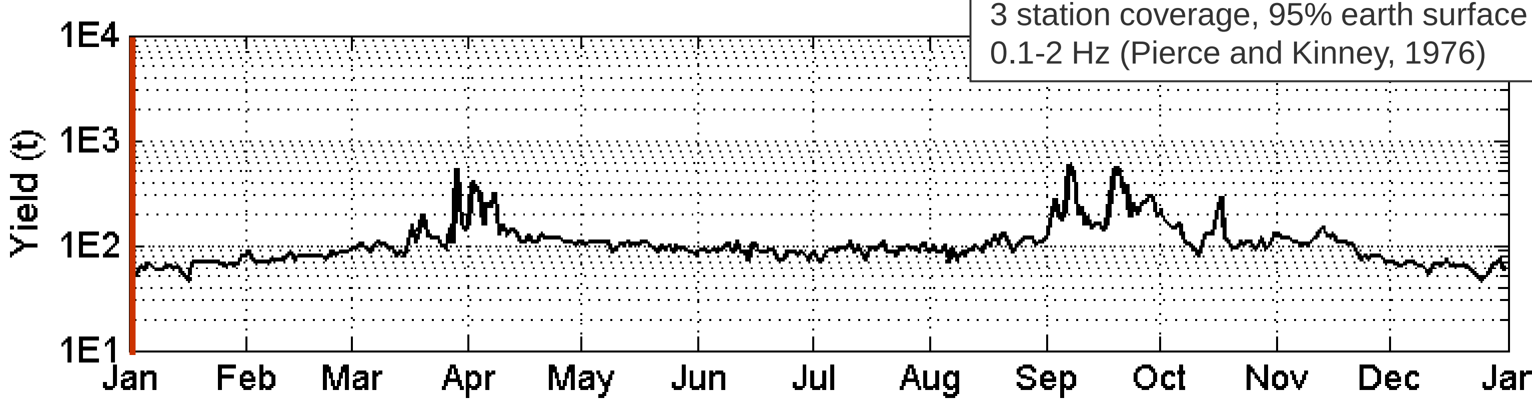

3 station coverage, 95% earth surface
0.1-2 Hz (Pierce and Kinney, 1976)

Assessing IMS network performance
Sayarim calibration experiment (January 2011)

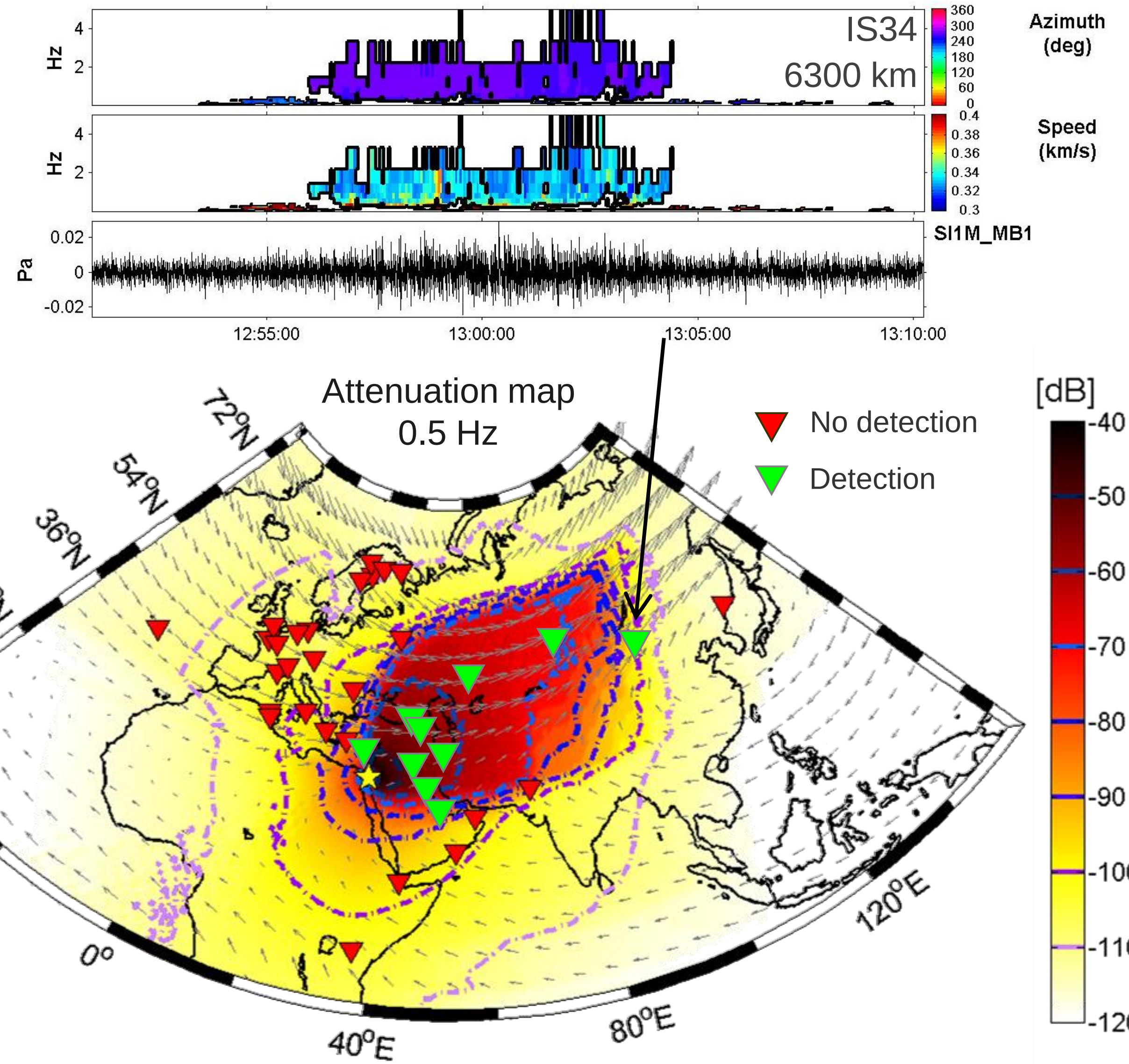

Participants : Geophysical Institute of Israël ; Geophysical Institute of Alaska, US; Univ. Mississipi, US; Univ. Hawaii, US; National Observatory, Athens; University of Firenze; CEA/DASE

Fee, D., et al. (2013), Overview of the 2009 and 2011 Sayarim Infrasound Calibration Experiments, J. Geophys. Res. Atmos., doi: 10.1002/jgrd.50398.

Infrasound radiated by industrial explosions
Propagation along unexpected paths

Gerdec, Albania (41.4N, 19.6E)
2008, March 15

Station	Range (km)
I26DE	950
I48TN	1096
IGADE	1554
DIA	1580
I31KZ	3113
I46RU	4917

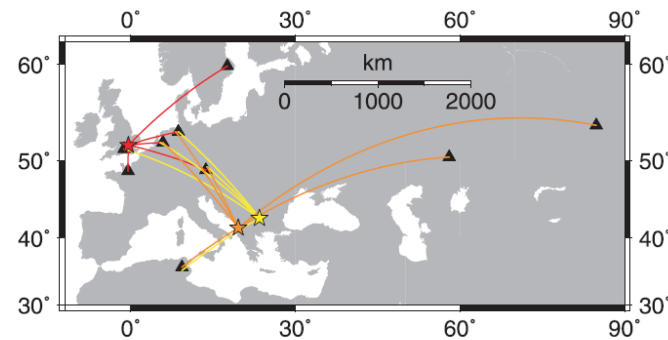

Green et al., JGI, 2011

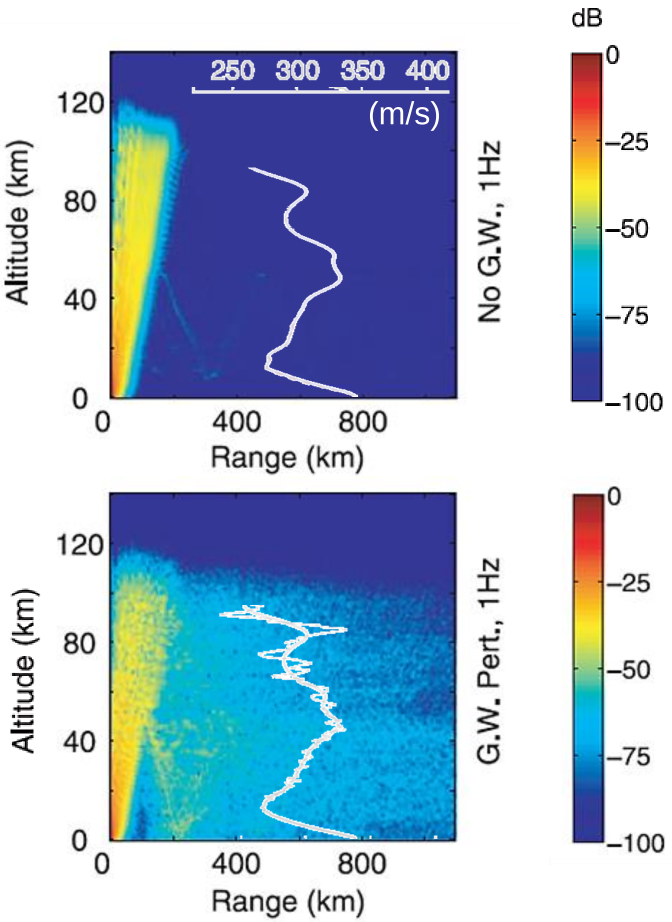

I48TN – 1096 km

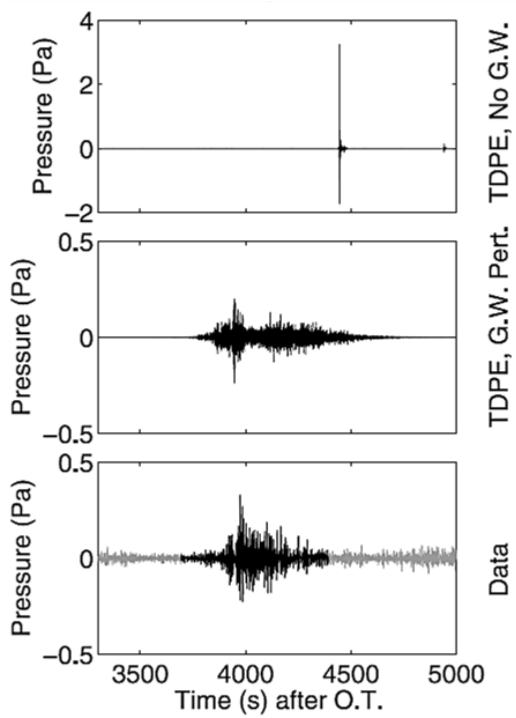

- ❑ Lack of resolution of state-of-the-art meteorological specifications
- ❑ Indicate that either weak, or no, ground-to-stratosphere waveguide (ECMWF)
- ❑ Parametrization of atmospheric fine-scale structures are lacking
- ❑ Incorporating gravity-waves into time-domain Parabolic Equation model predict observations

➔ Empirical approach to adjust wind corrections

ECMWF: European Centre for Medium-Range Weather Forecast

Earthquake-generated infrasound

The coupling problem: from ground-motion to pressure field

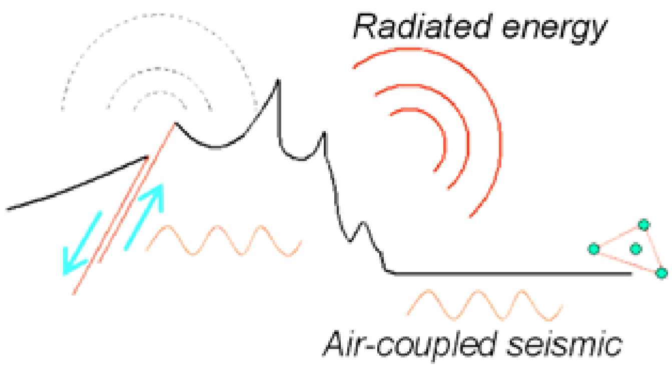

- Simulation of the 3C broadband seismograms
- Far-field approximation of the Helmholtz-Huygens integral
- Infrasound propagation using 3D ray-tracing

$$\frac{1}{2}p(\vec{r},t) = e^{-i\omega t}\iint_S \{p(\vec{r}_S,t)g_{,n}(\vec{r}-\vec{r}_S) - p_{,n}(\vec{r}_S,t)g(\vec{r}-\vec{r}_S)\}\,ds$$

$$p_\omega(\vec{r},t) = i\frac{k\rho c}{2\pi}\sum_{l=1}^{N} V(t_l)L_l\,\Delta h_l\,\frac{e^{-ik|\vec{r}-\vec{r}_l|}}{|\vec{r}-\vec{r}_l|}\,\frac{\sin(k\hat{x}_l L_l/2)}{k\hat{x}_l L_l/2}\,e^{-i\omega(t-t_l)}$$

Coupling →

Seismic Source —*Seismic Waves*→ Epicenter Land masses —*Infrasound Waves*→ Infrasound Array

- Source Parameters → Seismic Source
- Earth Velocity Structure → Seismic Waves
- Topographic Parameters → Epicenter Land masses
- Atmospheric Velocity Structure → Infrasound Waves
- Instrument Response → Infrasound Array

Topography → *Summation of adjacent strip line sources*

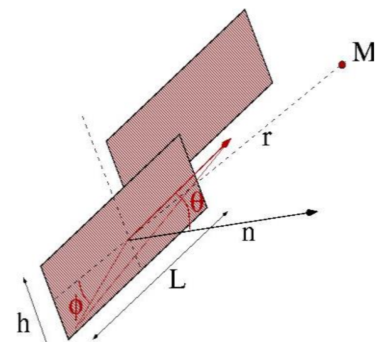

Donn and Posmentier, 1964
Young and Greene, 1982
Mutschlecner and Whitaker, 2005
Le Pichon et al., 2006, 2009

Earthquake-generated infrasound
Amatrice earthquake in central Italy, 24/08/2016 M6.2

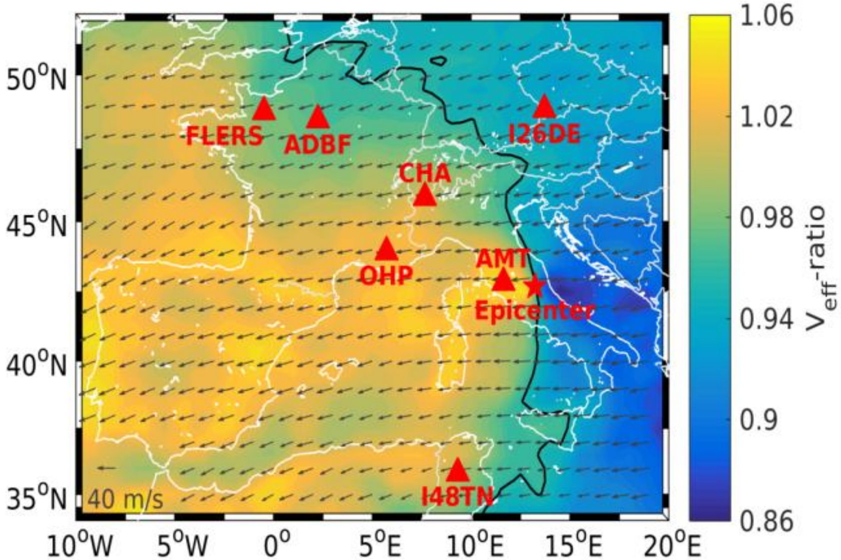

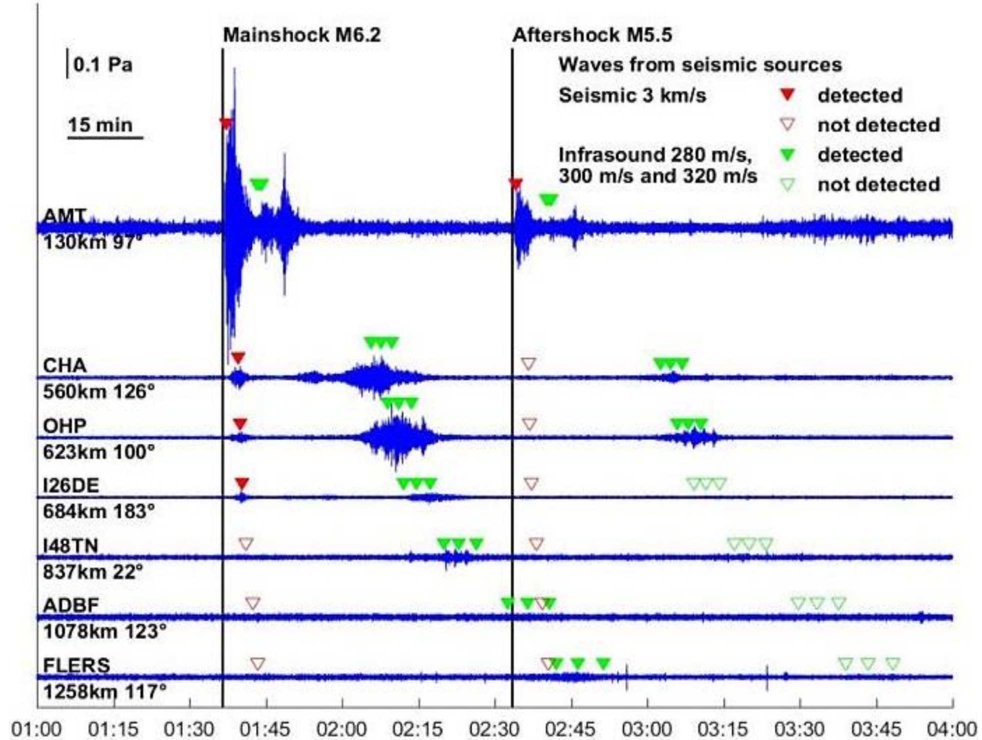

OHP, 623 km

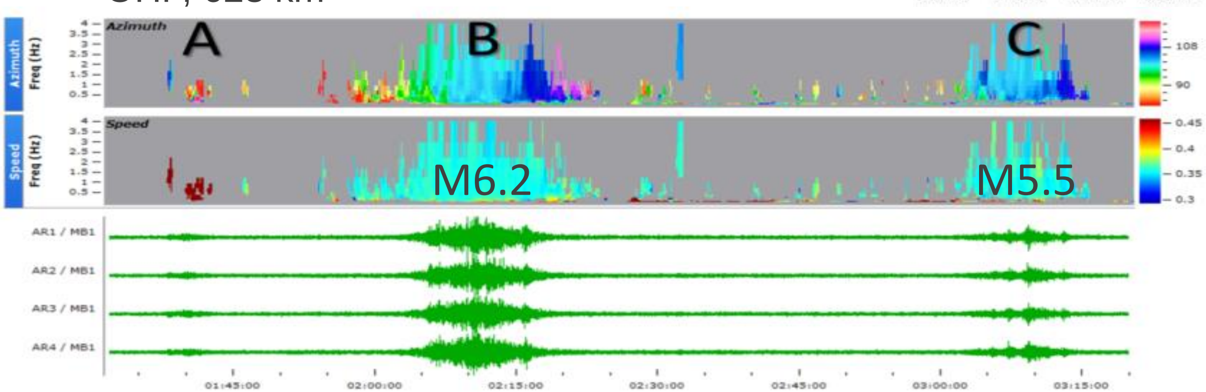

Recorded downwind by 7 infrasound arrays in the Euro-Mediterranean region at distances up to 1260 km.

Shani-Kadmiel et al., GRL, 2018
Hernandez et al., SRL, 2018 (in press)

Earthquake-generated infrasound
Amatrice earthquake in central Italy, 24/08/2016 M6.2

Surface pressure from ground motion measurements

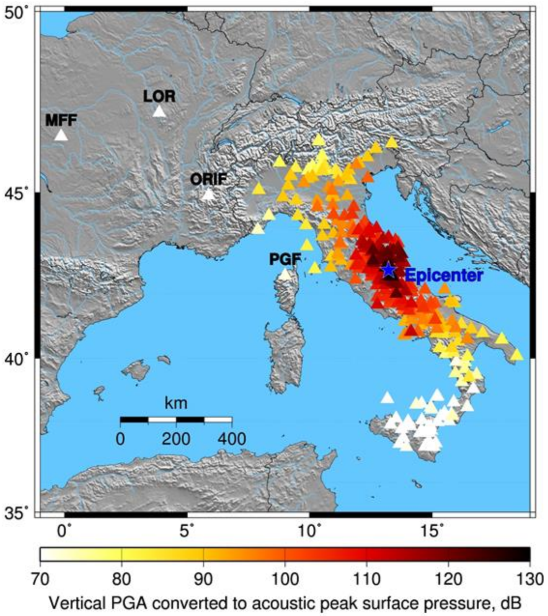

Surface pressure from infrasound measurements

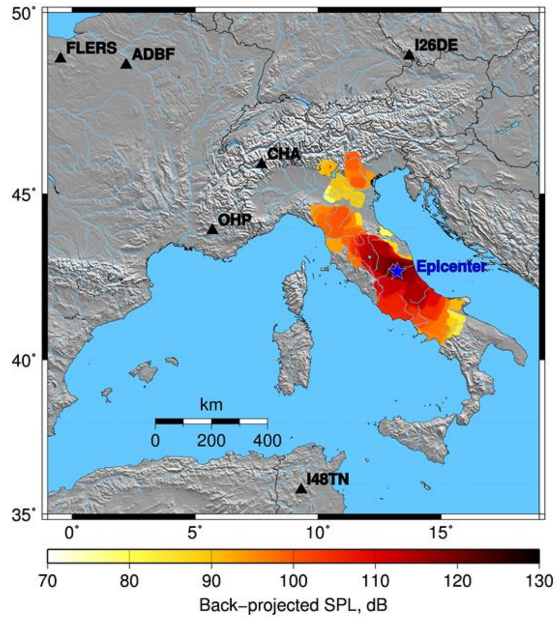

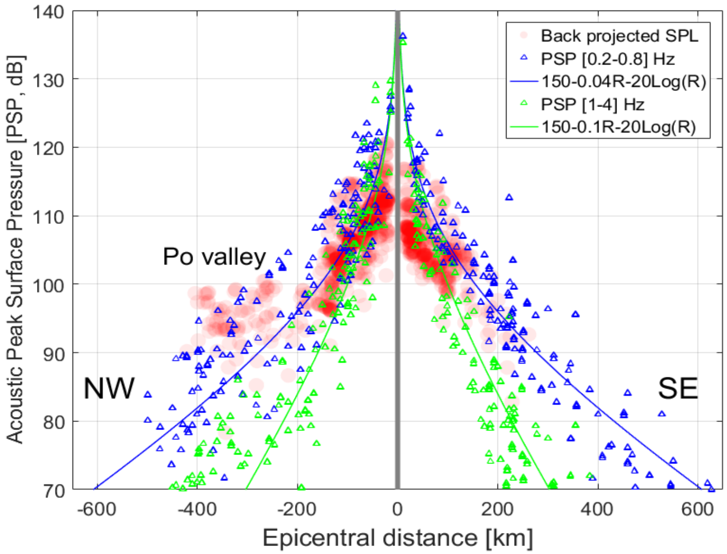

- The back projection of the infrasound illuminates radiating regions over ~600 km
- First order agreement between the acoustic surface pressure derived from infrasound records and the seismic source pressure derived from measured ground motion
- Infrasound records at hundreds of kilometers from moderate-magnitude earthquake can provide useful ground shaking information (local amplification caused by topographic and geological features)
- Improve procedures for shakemap estimation when surface observations are lacking

Shani-Kadmiel et al., GRL, 2018
Hernandez et al., SRL, 2018 (in press)

Outline

- ❑ Main challenges for infrasound interpretation
  - Highly variable atmospheric conditions
  - Improve knowledge on station signatures for discrimination
- ❑ Propagation and source studies
  - Using reference sources to assess atmospheric models
  - Network performance modeling
  - Earthquake generated infrasound
- ❑ Potential benefit for civil and scientific applications
  - Geophysical hazard warning systems
  - Developing atmospheric remote sensing method using infrasound
  - Towards a multi-technology approach to improve knowledge of the middle and upper atmosphere

Monitoring geophysical hazards
Infrasound from meteoroids

- Shock wave: Meteors generate infrasound during their entry in the Earth's atmosphere. Mach cones become cylinders and generate shock waves (ReVelle, 1976; 1997)
- Fragmentation: The high speed combined with an increasing atmospheric density, lead to thermal bursts. Energy of the explosions may reach kilotons TNT equivalent (Edwards, 2010)
- Propagation: Infrasound signals are refracted and channeled over long distances by the temperature gradient and the wind structure of the atmosphere

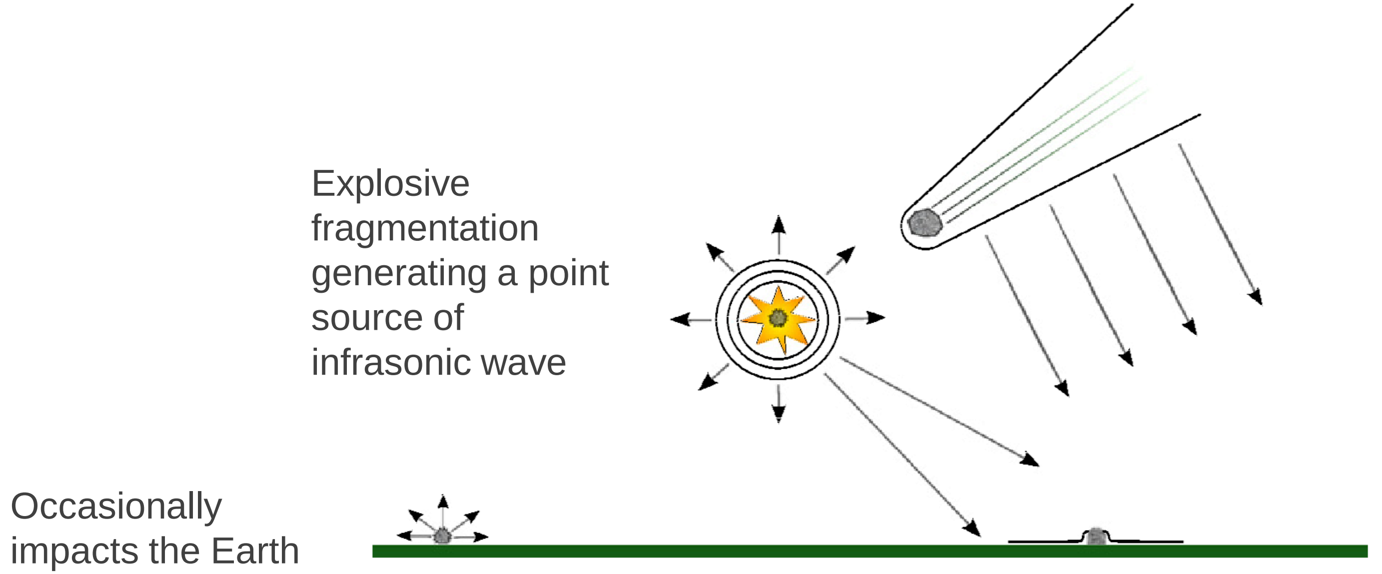

Adapted from Ens et al., 2012

Monitoring geophysical hazards
Chelyabinsk fireball, 15/02/2013

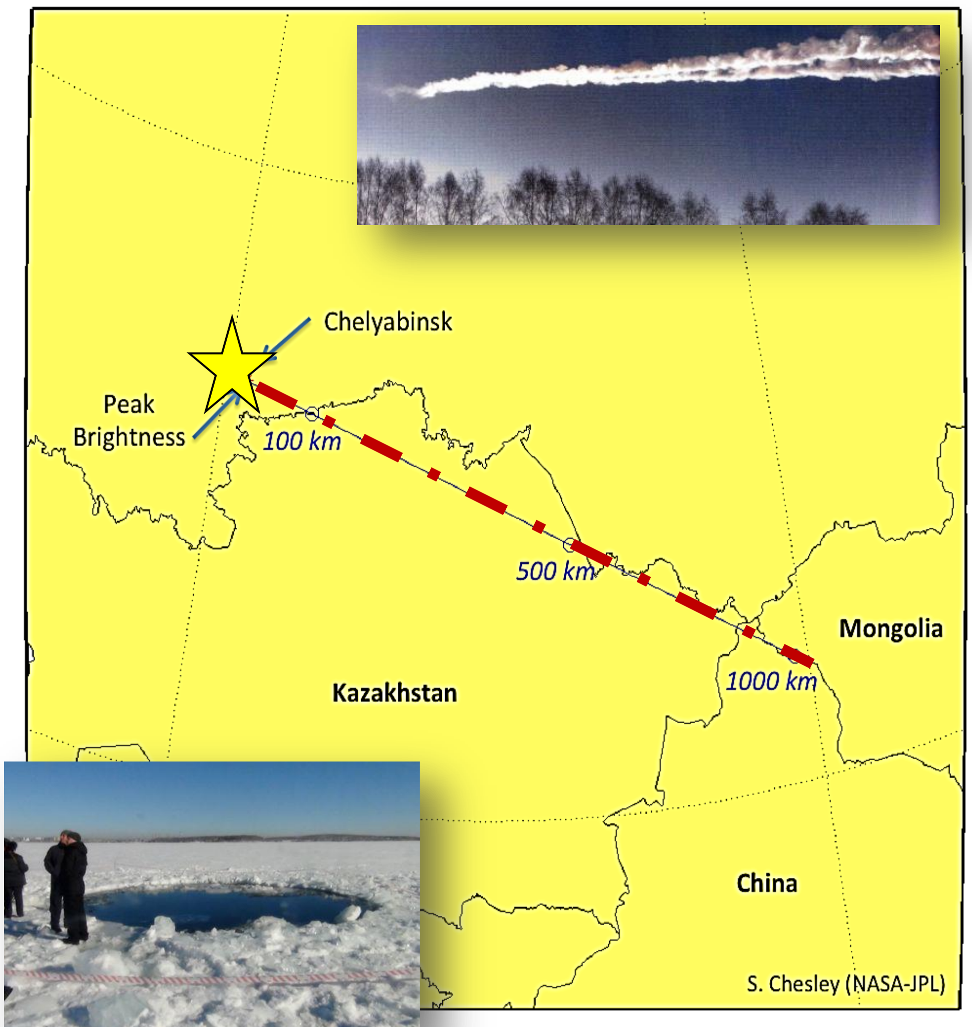

- On 15 February, 2013, a large Earth-impacting fireball entered the Earth's atmosphere over the Kazakh/Russia border
- Maximum brightness south of Chelyabinsk (54.80°N 61.10°E) near 30 km altitude
- A small asteroid at high speed (~20 km/s)
- Diameter: ~20 m, mass: ~15,000 t

Source: Univ. Western Ontario, Canada
http://www.nasa.gov/mission_pages/asteroids/news/asteroid20130215.html

Monitoring geophysical hazards
Chelyabinsk fireball, 15/02/2013

Most energetic event being instrumentally recorded

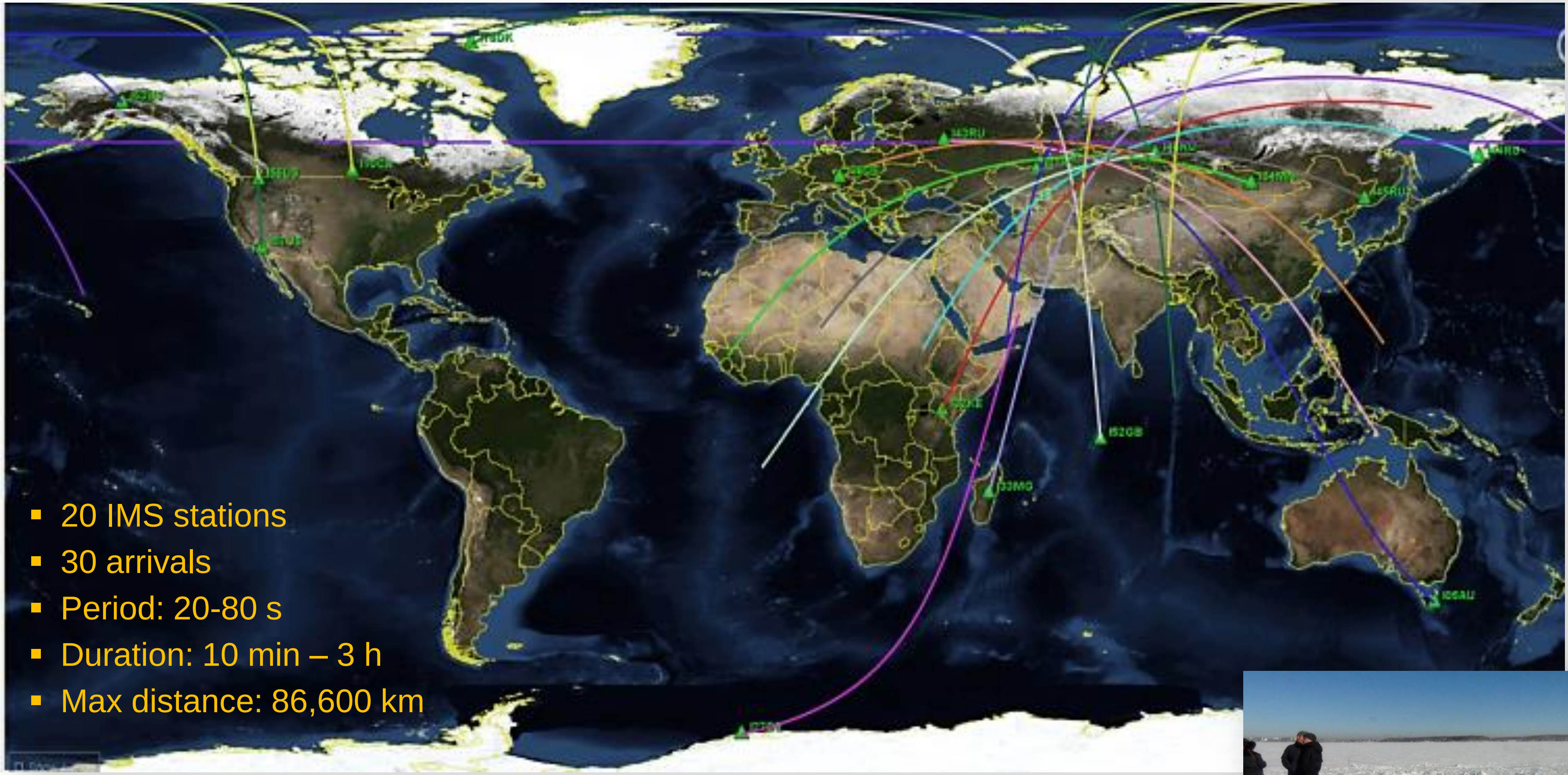

- 20 IMS stations
- 30 arrivals
- Period: 20-80 s
- Duration: 10 min – 3 h
- Max distance: 86,600 km

Monitoring geophysical hazards
Chelyabinsk fireball, 15/02/2013

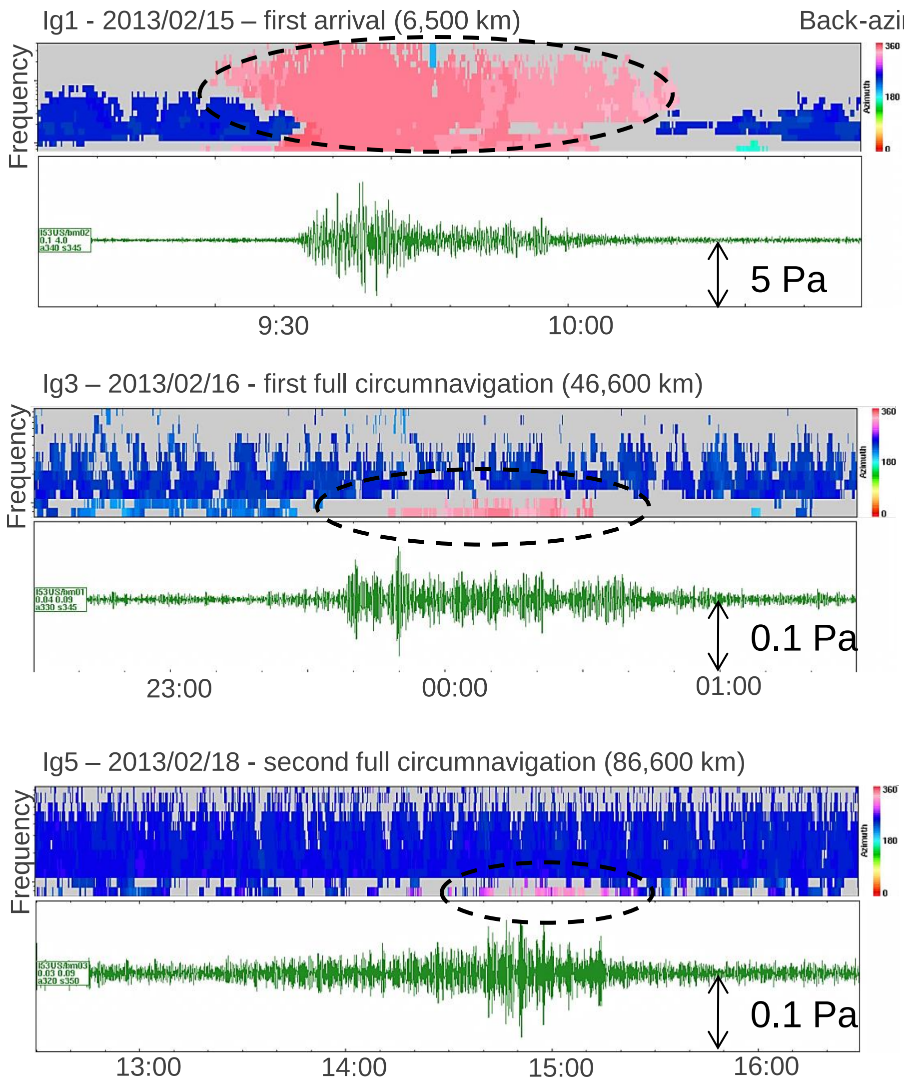

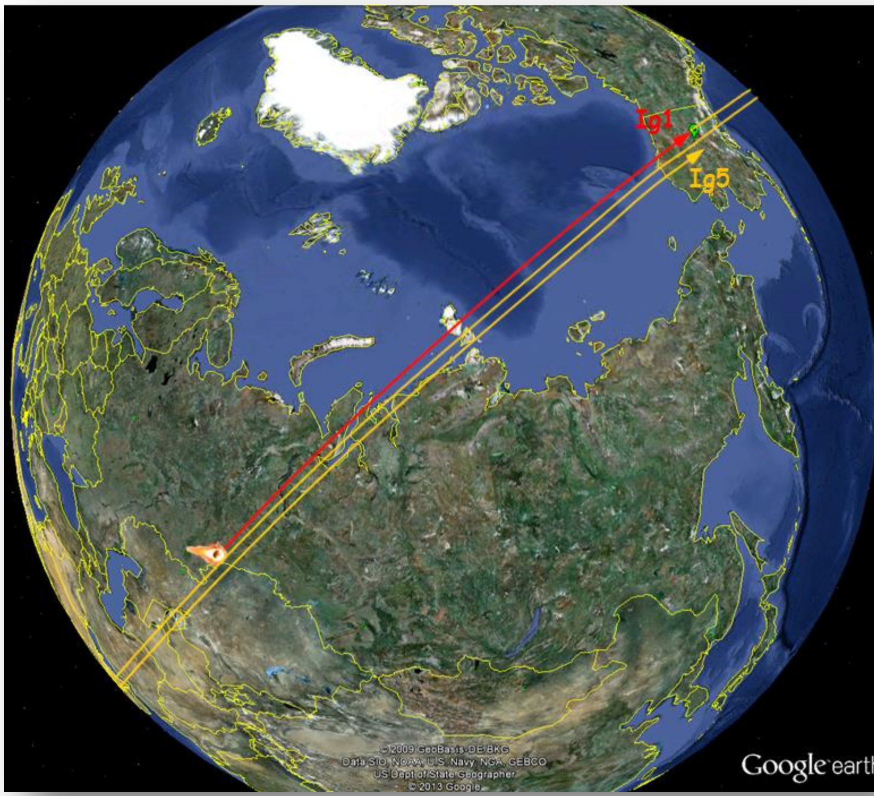

- ❑ Decrease of signal frequency with distance
- ❑ Almost no attenuation between Ig3 and Ig5

Monitoring geophysical hazards
Chelyabinsk fireball, 15/02/2013

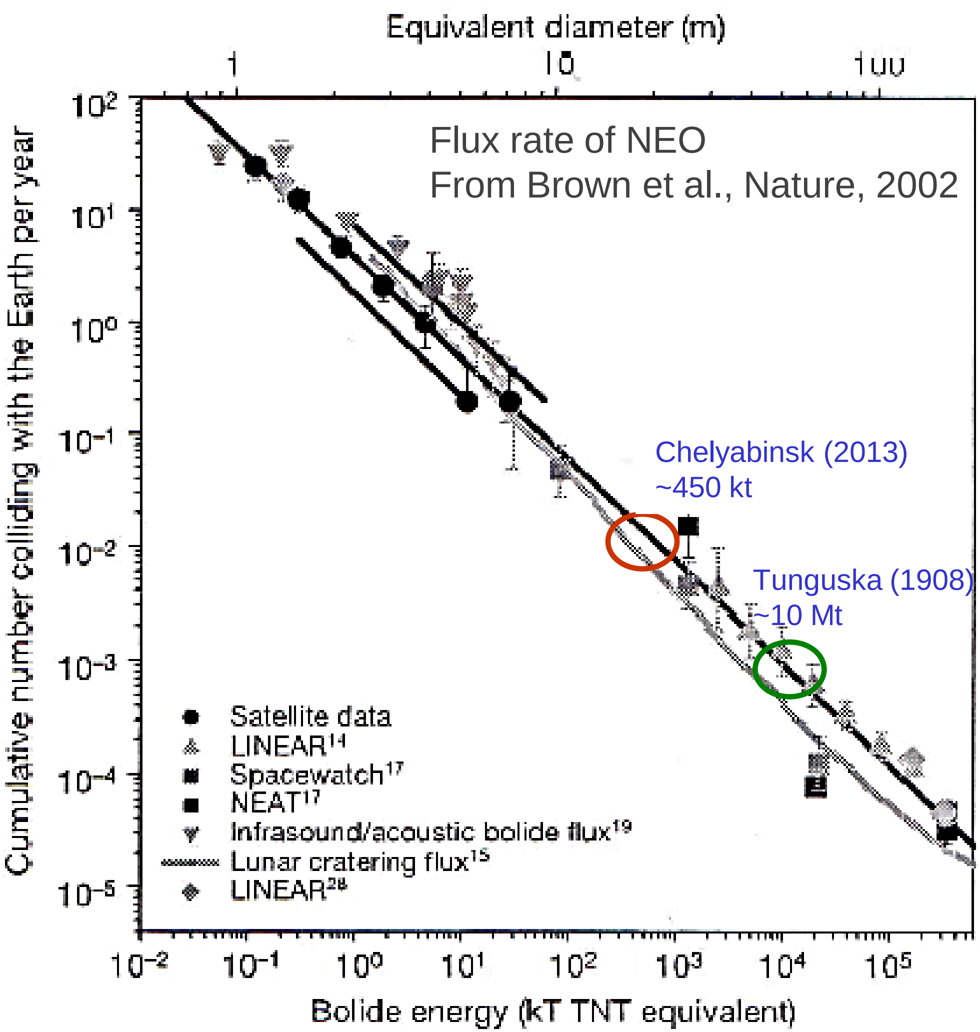

log W/2 = 4.14 log T - 3.61

U.S. Air Force Technical Center (AFTAC)

- ❑ Mean period: 40 s
- ❑ Explosive yield: ~450 kt of TNT
- ❑ Energy consistent with measured optical radiant energy (U.S. Government sensors)
- ❑ Expected to occur once every 100 years

➔ Infrasound provide additional constraints on source characteristic estimates for assessing meteor impact hazard

➔ A benchmark to assess global monitoring methods

Le Pichon et al., GRL, 2013
Brown et al., Nature, 2014

Volcanic hazards and aviation

Global flight paths

image: Michael Markieta
flight data: openflights.org

- ~1500 volcanoes worldwide active in the past 10,000 years
- Serious hazards to aircraft in flight near to the ash plume
- Many of the world's volcanoes lack dedicated monitoring instruments (e.g., bad weather, limited infrastructure, satellite coverage)

Siebert and Simkin, 2002
Global Volcanism Program, 2013

Monitoring geophysical hazards

Remote monitoring of volcanic eruptions

- Large scale volcanic eruptions may eject ash
- Ash encounters represent a serious threat to aircraft safety

Eyjafjallajökull eruptions, Island, April-May 2010

- Global detection of modest size eruption
- 15 detecting stations (1700-6000 km)
- Cross-bearing location at ~50 km from the volcano

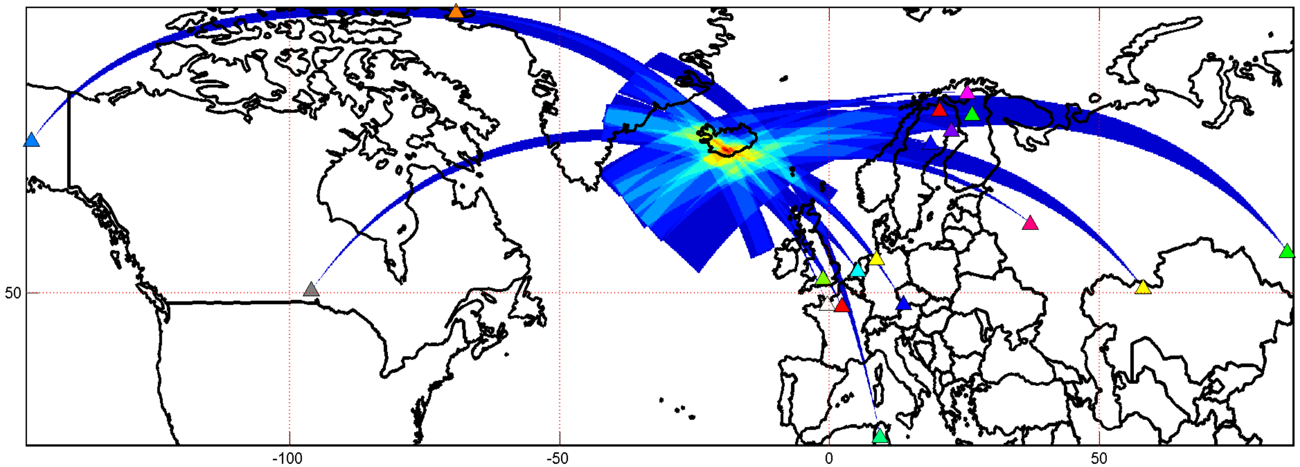

Matoza et al., GRL, 2011
Caudron et al., GRL, 2015

Monitoring geophysical hazards

Remote monitoring of volcanic eruptions

- Volcanic source terms are critical to model the ash dispersion
- Timely availability of reliable information is crucial to mitigate the risk of aircraft encountering volcanic ash (volcanic and seismological observatories, pilot report, remote sensing)
- Infrasound (<2Hz) may supplement other techniques for monitoring volcanic activity, especially in remote areas where that are poorly instrumented

Sarychev Peak eruption, Kuril Islands, 2009

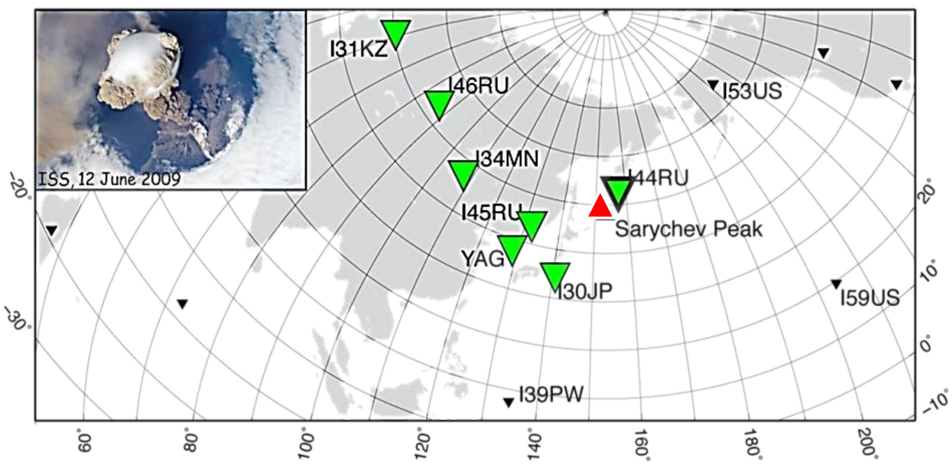

- Infrasound 640-6400 km from Sarychev Peak
- Sparse seismic network (remote location, no local monitoring)
- Infrasound data provide detailed explosion chronology with higher temporal resolution than satellite data

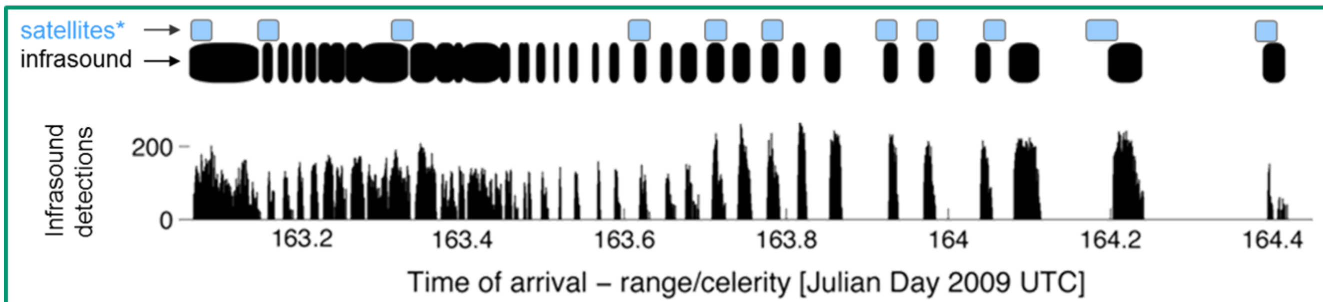

Matoza et al. (2011), Infrasonic observations of the June 2009 Sarychev Peak eruption, Kuril Islands: Implications for infrasonic monitoring of remote explosive volcanism, *J. Volcanol. Geotherm. Res.*

Monitoring geophysical hazards

Eruption of Calbuco, Chile - 22 April 2015


AGU PUBLICATIONS

JGR

Journal of Geophysical Research: Solid Earth

RESEARCH ARTICLE
10.1002/2017JB015182

Key Points:
- Calbuco 2015 eruption observed in local seismic (<15 km), regional seismo-acoustic (15–250 km), and remote acoustic data (>250 km) to 5,122 km
- Remote infrasound arrays provide accurate explosion chronology consistent with regional and local data and permit automated source location
- Regional seismo-acoustic networks augment the International Monitoring System and enhance volcanic signal detection

Local, Regional, and Remote Seismo-acoustic Observations of the April 2015 VEI 4 Eruption of Calbuco Volcano, Chile

Robin S. Matoza[1], David Fee[2], David N. Green[3], Alexis Le Pichon[4], Julien Vergoz[4], Matthew M. Haney[5], T. Dylan Mikesell[6], Luis Franco[7], O. Alberto Valderrama[7], Megan R. Kelley[1,8], Kathleen McKee[2], and Lars Ceranna[9]

[1]Department of Earth Science and Earth Research Institute, University of California, Santa Barbara, Santa Barbara, CA, USA, [2]Wilson Alaska Technical Center, Alaska Volcano Observatory, Geophysical Institute, University of Alaska Fairbanks, Fairbanks, AK, USA, [3]AWE Blacknest, Reading, UK, [4]CEA, DAM, DIF, Arpajon, France, [5]Alaska Volcano Observatory, U.S. Geological Survey Volcano Science Center, Anchorage, AK, USA, [6]Department of Geosciences, Boise State University, Boise, ID, USA, [7]Observatorio Volcanológico de los Andes del Sur, Servicio Nacional de Geologia y Minería, Temuco, Chile, [8]Now at Department of Earth and Planetary Sciences, University of California, Santa Cruz, CA, USA, [9]BGR, Hannover, Germany

- VEI 4, plume heights > 23 km
- >6,500 evacuated from local communities
- Detections at 11 IMS stations
- Timing estimates of explosive phases:
  - 22 April 21:04 UT, duration: 1.5 hours
  - 23 April 04:00 UT, duration: 6.2 hours

[Van Eaton et al., 2016]

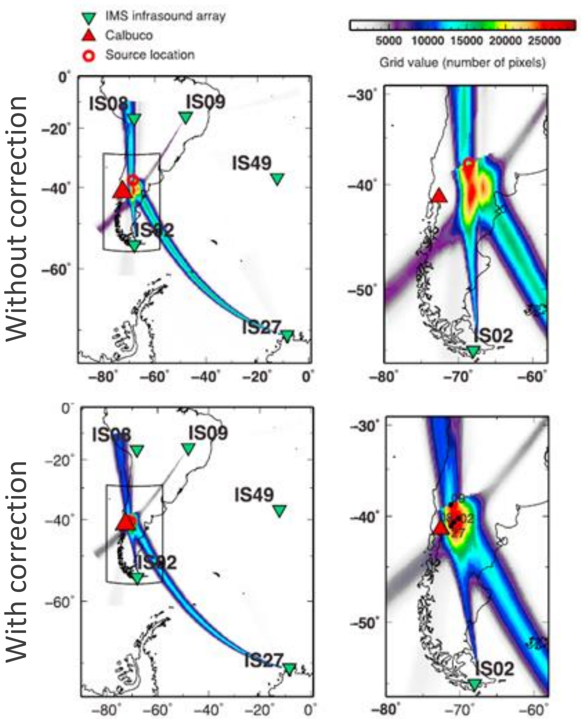

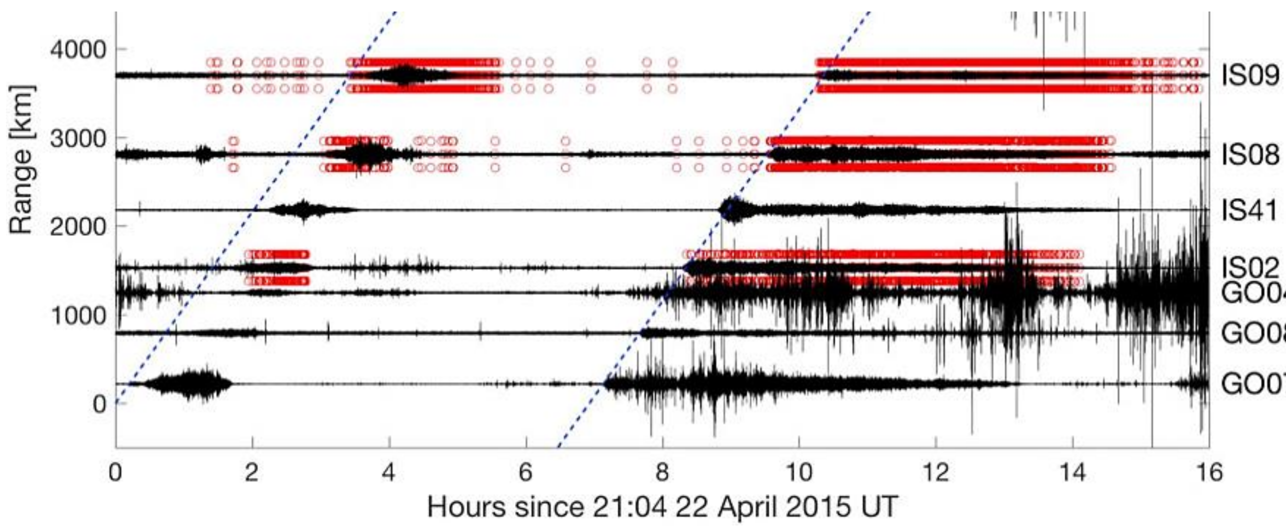

From science to operations
Where infrasound can help the VAACs

- Infrasound supplement other techniques for monitoring volcanic activity, especially in remote areas that are poorly instrumented
- The proposed approach is tested with Toulouse VAAC, mandated by ICAO, to demonstrate the usefulness of IMS data to IAVW

Toulouse Volcanic Ash Advisory Center
Aviation code: red

Info source : INGV, webcam, satellite imagery

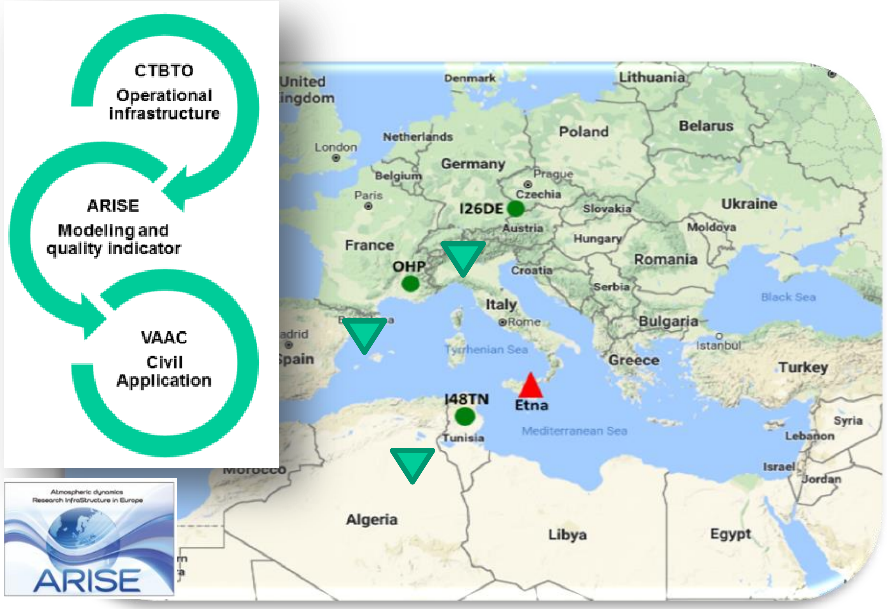

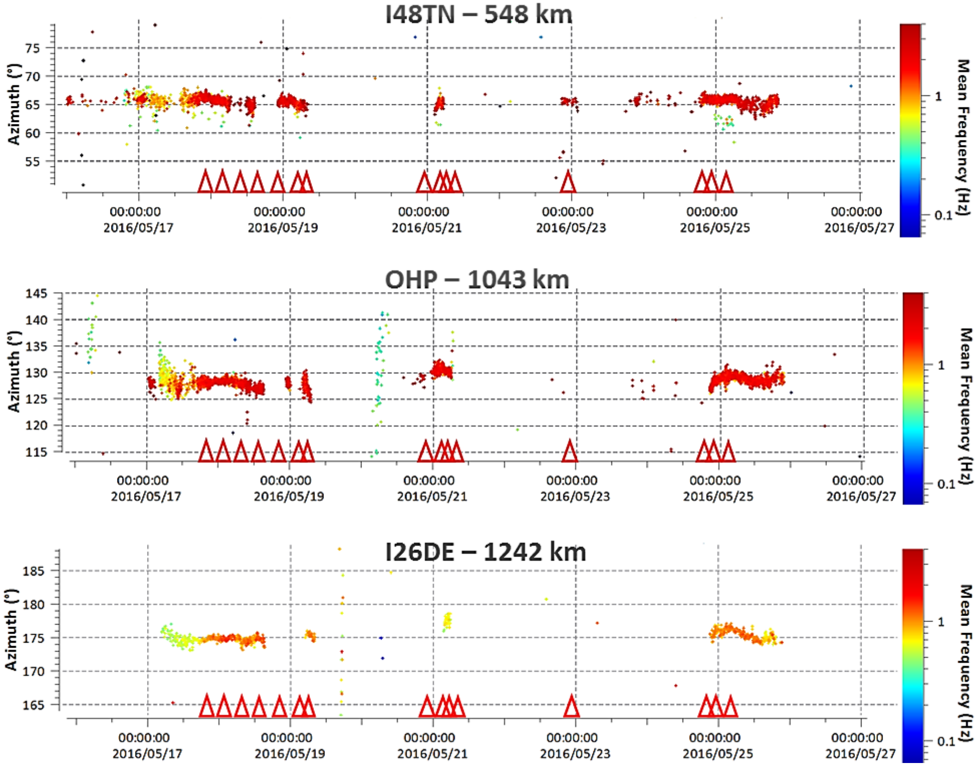

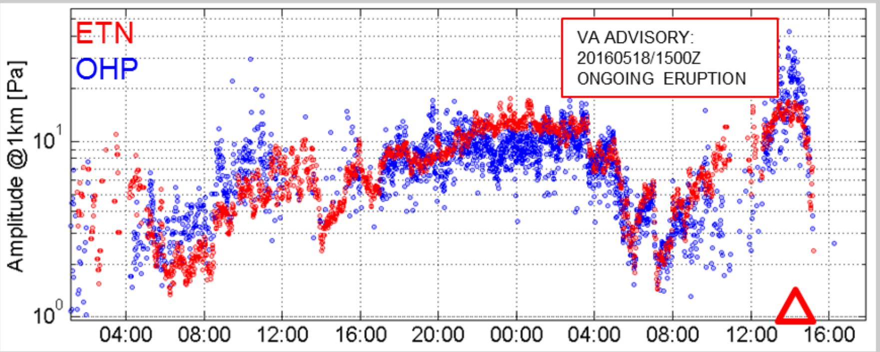

Developing atmospheric sensing methods using volcano infrasound

Developing atmospheric sensing methods using volcano infrasound

Microbarometer near Yasur (~200 m)

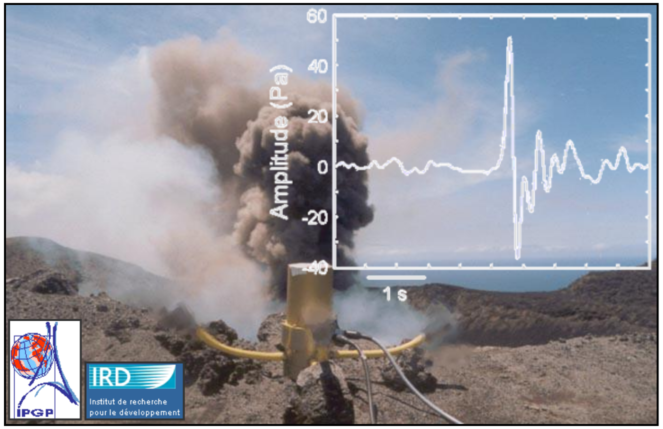

Station I22FR (~400 km from Yasur)

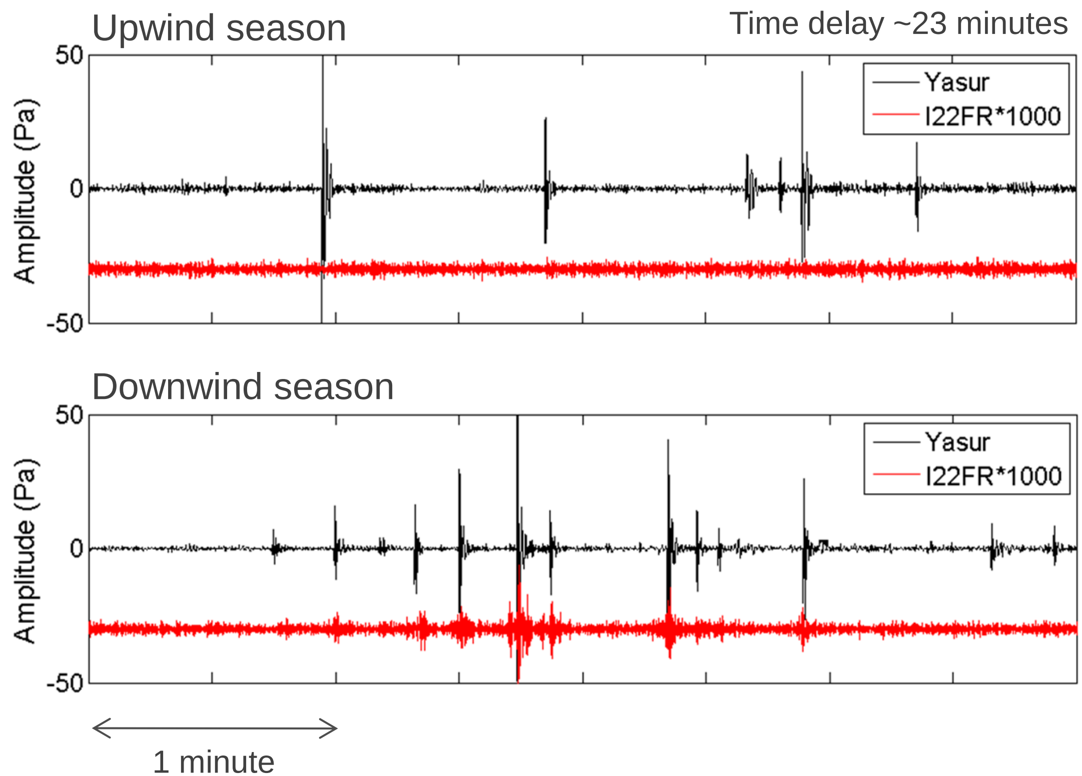

- ❑ Time sequences in near and far field correlate well during downwind season
- ❑ ~60 dB attenuation

Vergniolle et al., 1996

Developing atmospheric sensing methods using volcano infrasound

Measuring planetary waves (Yasur)

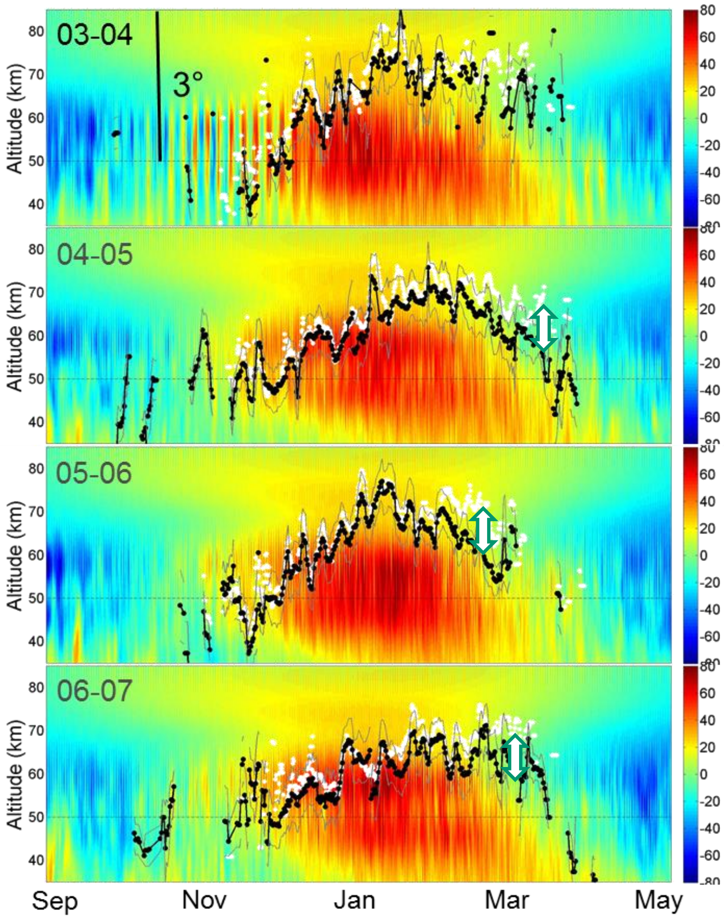

~5 day oscillations associated to large scale planetary waves (Antier et al., JGR, 2007)

Evaluating tidal oscillations (Yasur)

-- Observations
-- Simulations

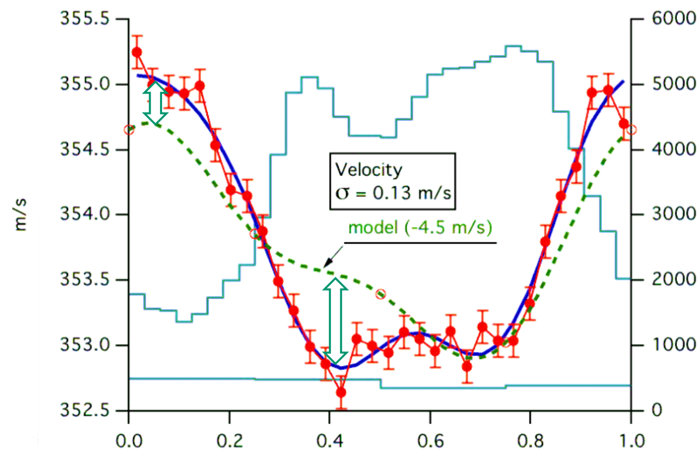

- ❑ Observed diurnal oscillations (~1° and ~4 m/s)
- ❑ Underestimated by ~10 m/s tidal oscillations of the meridional winds at 50 km (ECMWF)

(Dalaudier et al., EGU, 2009)

Evaluating wind speed in the mesosphere / lower thermosphere (MLT)

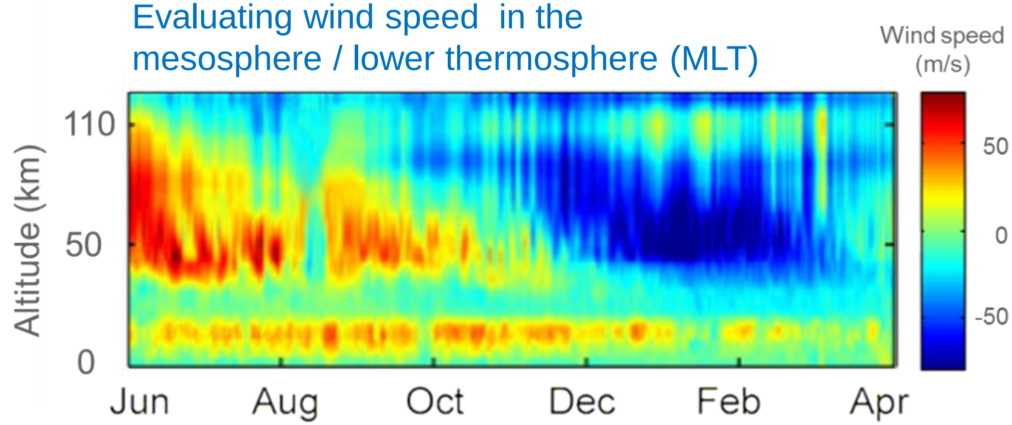

- ❑ Reconstruct stochastic variations in the MLT; mesospheric wind jets generally underestimated (Le Pichon et al., JGR, 2005; 2006)
- ❑ Formalism for iterative linear inversion procedure (Lalande et al., JGI, 2011; Assink et al., JGR 2015)

ARISE
Atmospheric dynamics Research InfraStructure in Europe

ARISE Project

A multi-technology platform to better characterize middle and upper atmospheric dynamics

- Collaborative Infrastructure project (H2020), http://arise-project.eu
- 24 partners, coordinated by CEA (France)
- Objectives:
  - Comparing global circulation model products with independent MA measurements
  - Quantifying bias observed in the stratospheric region due to physics parametrization of the IFS and the existence of the sponge layer
  - Characterizing gravity waves perturbations filtered out by the models (period, amplitude, vertical wavelength)

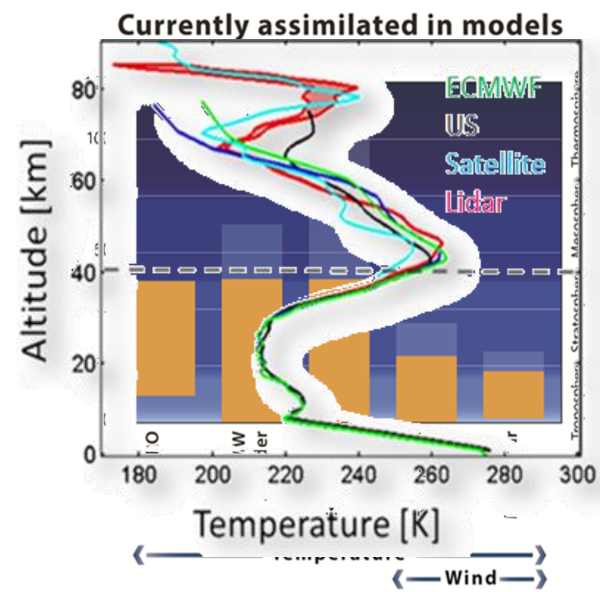

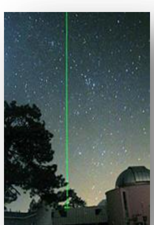

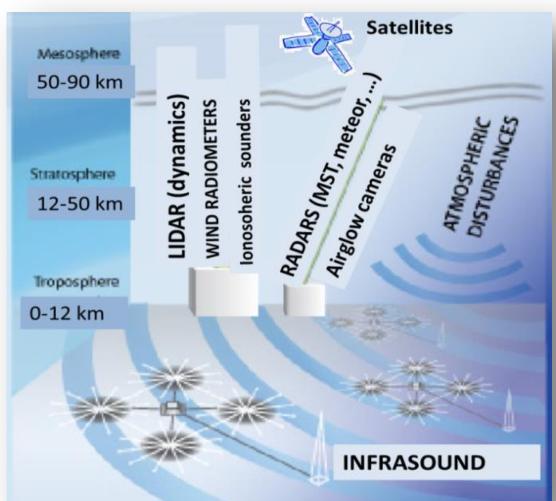

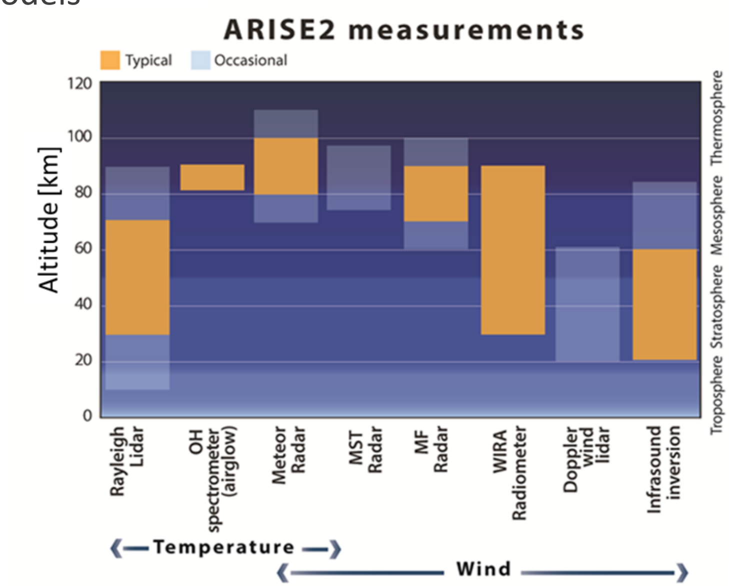

Towards a multi-technology infrastructure

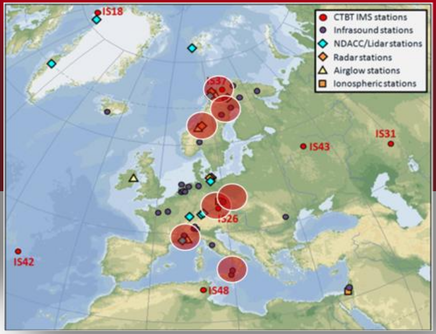

Comparing high-resolution lidar sounding with NWP models in the midlle atmosphere

- ALOMAR (Andøya, 69.3N 16.0E): Arctic Lidar Observatory for Middle Atmosphere Research: Lidar Iron doppler / RMR + Meteor radar
- ~10 minutes temporal resolution, instrumental error < 5K and 5 m/s
- Observation of quasi-monochromatic gravity waves (T>6h), ~1-10 km vertical wavelength
- Large amplitudes (±20K and 40 m/s at 40 km) underestimated by empical models
- Need to better parameterize unresolved wind perturbations
  - ➔ Infrasound monitoring
  - ➔ Atmospheric community

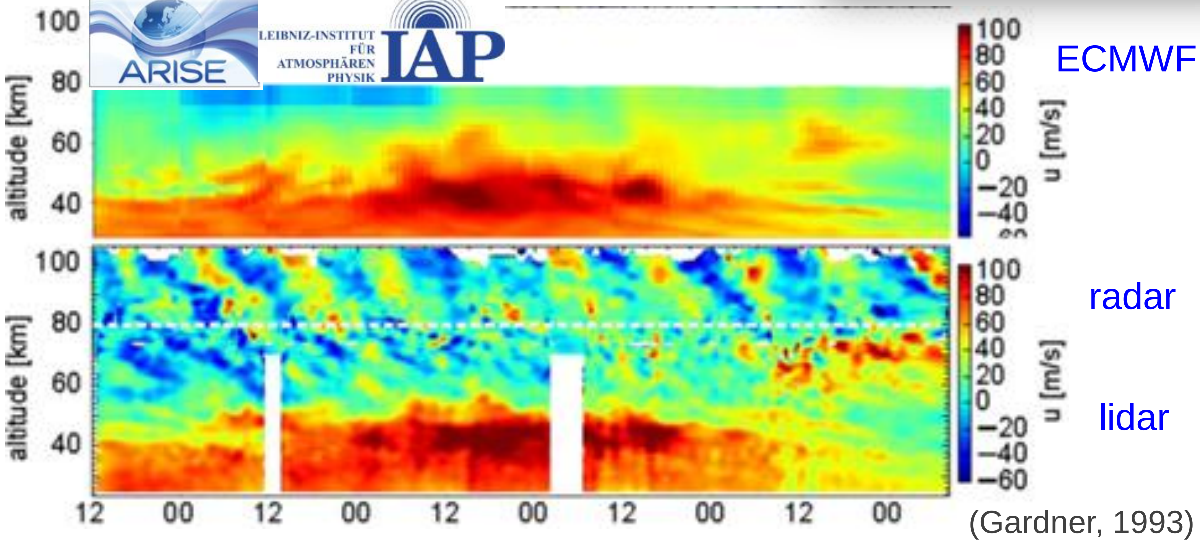

(Gardner, 1993)

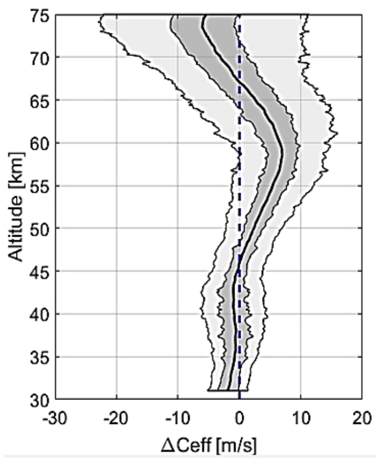

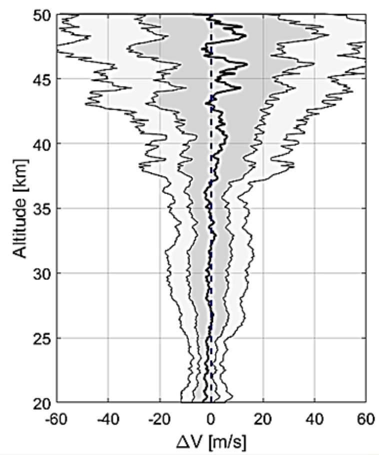

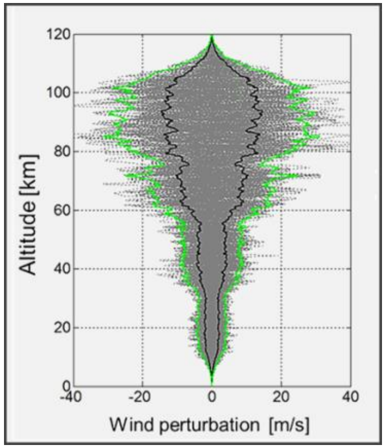

Summary

Lessons learnt from operational monitoring

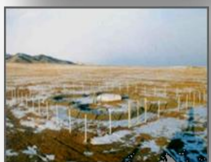

- A global coverage of infrasound
  - Strong increase in the number of operating stations and reference events
  - Larger and much more sensitive than any previously operated network
  - Benchmark to assess/optimize operational procedures
- Advances in operational monitoring methods
  - A broad spectrum of coherent signals
  - Better discrimination between interfering signals
  - Improved knowledge of station signature
  - High-resolution network performance modeling
- Potential benefits for civil and scientific applications, supplements other techniques for monitoring natural hazards
  - Constraints for assessing meteor impact hazard
  - Remote estimation of areas of strong ground motions
  - Reliable information for volcanic hazard warning systems (CTBTO, VAACS)
  - Develop operational procedures to routinely evaluate NWP models
  - Towards assimilation to improve resolution of weather and climate models